A

39

AD A113914

⑫

the ohio state university

research foundation
1314 kinnear road
columbus, ohio
43212

T-MATRIX FORMULATION TO STUDY THE FREQUENCY DEPENDENT
PROPERTIES OF ABSORBING MATERIALS

V. K. Varadan and V. V. Varadan
Department of Engineering Mechanics

For the Period
August 1, 1980 - October 31, 1981

DTIC FILE COPY

DTIC
SELECT
S
APR 28 1982
E

January 15, 1982

82 04 16 062

CO 703.53

COHERENT WAVE ATTENUATION AND FREQUENCY DEPENDENT
PROPERTIES OF ABSORBING MATERIALS

by

Vijay K. Varadan and Vasundara V. Varadan
Wave Propagation Group
Department of Engineering Mechanics
The Ohio State University, Columbus, Ohio 43210

September 1981

Abstract

A scattering matrix theory is presented for studying the multiple scattering of both longitudinal and transverse elastic waves in a medium containing a random distribution of inclusions or voids of arbitrary shape. A statistical analysis with QCA and Percus-Yevick pair correlation function is then employed to obtain expressions for the average amplitudes of the coherent fields which may be solved to yield the bulk or effective properties of the inhomogeneous medium. Suggestions for incorporating CPA in conjunction with QCA so that materials with dense concentration of inclusions can be considered are also given.

Introduction

In recent years, considerable effort has been devoted to promoting the development of elastomeric absorbing materials, containing a distribution of cavities and inclusions, which are bonded to submerged structures to control the sound radiated by these structures as well as to modify their acoustic reflection characteristics (echo reduction). To use such absorbing layers, it is important to determine how their physical properties such as density, thickness and effective elastic moduli, and material composition such as distribution and orientation of the inclusions and their size distributions affect the acoustical behavior of any actual sturcture coated with that material.

The waves incident on such inhomogeneous media undergo multiple scattering due to the presence of inclusions thus reducing the scattering amplitude or cross section by absorption and attenuation of waves. The attenuation depends critically on the material properties of the host medium (matrix) and inclusions, the distribution of the inclusions and the frequency of the incident wave. The problem is very difficult and to our knowledge, rigorous theories with numerical results are not available in the literature.

In multiple scattering theories, approximations are usually made at a very early stage for a) the geometry of the inclusion, b) the size of the inclusion relative to the wavelength of incident wave, and c) distribution of the inclusions in the matrix medium. The approximations with respect to geometry and size are related. If the inclusion is small compared to the incident wavelength, it is not possible to "see" exact

details of the inclusion and usually one is content to obtain the gross
scattering properties of the inhomogeneous medium. This is the so-called
Rayleigh or low frequency limit, and yields corrections to the solution
for point scatterers. As far as the distribution of the inclusions is
concerned, one either has regular arrays of inclusions or a random
distribution. In the former case, one performs a lattice sum while in
the latter case, one employs a configurational averaging procedure. If
the concentration of inclusions is small, i.e., the inclusions are sparsely
distributed, we may use a single scattering or first Born approximation.
Approximations have been employed by many authors and the corresponding
effective properties of the medium were studied at the low frequencies and
low concentrations, see for example, Waterman and Truell [1], Merkulova [2],
Chaban [3,4], Chatterjee and Mal [5], Domany, Gubernatis and Krumhansl [6],
Korringa [7], Kröner [8], Datta [9] and the references therein. Actually
the real problem warrants a rigorous multiple scattering theory and a
computational approach to study the frequency dependent properties of the
inhomogeneous media which will be valid for frequencies comparable to
scatterer size and for a wide range of concentrations, shapes and sizes.

Recently, the present investigators have developed a multiple scattering
formalism by introducing the concept of a T-matrix for individual inclusions
that makes the formulation more general and applicable to a variety of
different scatterers, see Refs. [10-20]. The method also lends inself to
numerical computations for higher frequencies of the incident plane wave as
well as more realistic geometries for the inhomogeneities. The dynamic
elastic properties of composite elastic media have been studied in [20]
using this formulation, and the concept of an average frequency dependent

elastic stiffness tensor following the work of Bedeaux and Mazur [21], and Varadan and Vezetti [22]. The results seem to be promising for future research in this area. In Ref. [20], we have shown that a Clausius-Mosotti type formula for the average shear modulus can be recovered in the low frequency limit. For higher frequencies, we have obtained the dynamic properties for a range of frequencies. The extension of the theory presented in [20] to acoustic and elastic wave scattering will be useful for Naval applications.

The present state of the art is as follows: the statistical considerations seem to be the most difficult for three dimensional inclusions and the least amount of progress has been made in this area. All formalisms that involve ensemble averaging result in a heirarchy of equations for the average fields that involve higher and higher order correlation functions. This heirarchy must be truncated in some fashion. Foldy [23] approximated the field incident on a scatterer by the average field itself. Lax [24] was the first to use a quasi-crystalline approximation which involves the two particle correlation function. At the moment, only the 'hole correction' has been taken into account in a systematic way. Bose and Mal [25] have tried correlation functions that fall off exponentially with distance. Recently, Twersky [26] has used the scaled particle equation of state of a gas of hard spheres to obtain improvements to the hole correction integral. The T-matrix formalism employs Lax's quasicrystalline approximation (QCA), the hole correction integral and results in a set of equations that must be solved in a self-consistant manner.

In this paper, a radially symmetric pair-correlation function given by Percus-Yevick (P-YA) integral equation [27] is introduced which gives

improvements to the hole correction integral. The "well-stirred" approximation (WSA) was used previously by us which assumes no correlation between the scatterers except that they should not interpenetrate. The WSA seems to depend on concentration and frequency. At low frequency or Rayleigh limit, WSA gives good results up to concentration, $c \leq 0.04$ and unphysical results for $c \geq 0.125$ [28], However, at higher frequencies and higher concentration, the WSA with quasi-crystalline approximation (QCA) yields better results. At resonance frequencies we note that P-YA is so far the appropriate correlation function to be employed [29-31].

Formulation of the Problem

Consider N identical, finite elastic inclusions that are randomly distributed in a different elastic medium, see Fig. 1. The scatterers are homogeneous with elastic properties given by Lame's constants λ_1 and μ_1 and density ρ_1. The properties of the outside medium (call matrix) are given by λ, μ and ρ. In Fig. 1, 0_i and 0_j refer to the center of the i-th and j-th scatterers, respectively and they are referred to the origin 0 by the spherical polar coordinates (r_i, θ_i, ϕ_i). P is any point in the medium outside the scatterers (the matrix medium).

A time harmonic plane wave of unit amplitude and frequency ω is incident on the medium such that the direction of propagation of the incident waves is along the z-axis, which may be written in terms of displacement field vector $\vec{u}^0$:

$$\vec{u}^0(\vec{r}) = e^{i(k_p z - \omega t)\hat{z}} + e^{i(k_s z - t)\hat{x}} \qquad (1)$$

where k_p and k_s are the compressional and shear wave numbers given by

$$k_p = \omega/c_p \quad ; \quad c_p = \sqrt{(\lambda + 2\mu)/\rho} \tag{2}$$

$$k_s = \omega/c_s \quad ; \quad c_s = \sqrt{\mu/\rho} \tag{3}$$

and t is the time. The waves incident to the discrete random media will undergo multiple scattering. Let $\vec{u}_i^s(\vec{r})$ be the field scattered by the i-th scatterer. The incident and scattered fields satisfy the vector Helmholtz equation. The problem at hand reduces to computing the total wave field at any point in the matrix medium and hence the bulk properties, satisfying the appropriate boundary condition on the surface of the scatterers and radiation conditions at infinity.

The total field at any point in the matrix medium can be interpreted as the sum of the incident field and the fields scattered by all the scatterers, which can be written as

$$\vec{u}(\vec{r}) = \vec{u}^0(\vec{r}) + \sum_{i=1}^{N} \vec{u}_i^s(\rho_i) \quad ; \quad \vec{\rho}_i = \vec{r} - \vec{r}_i \quad . \tag{4}$$

However, the field that excites the i-th scatterer is the incident field $\vec{u}^0$ plus the fields scattered from all other scatterers except the i-th. The term exciting field $\vec{u}^e$ is used to distinguish between the field actually incident on a scatterer and the external incident field $\vec{u}^0$ produced by a source at infinity. Thus, at a point $\vec{r}$ in the vicinity of the i-th scatterer, we write

$$\vec{u}_i^e(r) = \vec{u}^0(\vec{r}) + \sum_{j \neq i}^{N} \vec{u}_j^s(\vec{\rho}_j) \quad ; \quad a \leq |\rho_j| < 2a \tag{5}$$

where 'a' is a typical dimension of the scatterer.

The exciting and scattered fields for each scatterer can be expanded in terms of vector spherical functions with respect to an origin at the center of that scatterer:

$$\vec{u}_i^e(\vec{r}) = \sum_{\tau=1}^{2} \sum_{\ell=1}^{\infty} \sum_{n=0}^{\ell} \sum_{\sigma=1}^{2} b_{\tau\ell n\sigma}^i \, \text{Re} \, \vec{\psi}_{\tau\ell n\sigma}(\vec{\rho}_i) = \sum_{\tau n} b_{\tau n}^i \, \text{Re} \, \vec{\psi}_{\tau n}^i \qquad (6)$$

$$\vec{u}_i^s(\vec{r}) = \sum_{\tau n} B_{\tau n}^i \, \vec{\psi}_{\tau n}^i \qquad (7)$$

where $\vec{\psi}_{\tau\ell n\sigma}$ ($\tau = 1,2,3$) are the vector spherical vector basis functions [19]. Field quantities that are regular at the origin are expanded in terms of the regular (Re) basis set (Re $\vec{\psi}_{\tau\ell n\sigma}$) obtained by replacing the Hankel function of the first kind, h_n, in the above equations by the spherical Bessel functions j_n of the first kind. In Eq. (7), we abbreviate these vector basis functions as $\vec{\psi}_{\tau\ell n\sigma} = \vec{\psi}_{\tau n}$. We note that $\vec{\psi}_{1n}$ is for the longitudinal part while $\vec{\psi}_{2n}$ and $\vec{\psi}_{3n}$ for the transverse parts. The choice of the basis set in Eq. (7) satisfies the radiation condition at infinity for the scattered field, while the choice in Eq. (6) satisfies the regular behavior of the exciting field in the region $a < |\vec{\rho}_i| < 2a$. The superscript i on the basis functions refer to expansions with respect to 0_i, and $b_{\tau n}^i$ and $B_{\tau n}^i$ are the unknown exciting and scattered field coefficients. We also expand the incident field in terms of vector spherical functions:

$$\vec{u}^0 = \frac{e^{i k_p \zeta_i}}{i k_p} \sum_{s=0}^{\infty} \sum_{t=-s}^{s} (2s + 1) i^s \operatorname{Re} \vec{\psi}^i_{1ts} \delta_{t,0}$$

$$+ \frac{1}{2i} e^{i k_p \zeta_i} \sum_{s=1}^{\infty} \sum_{t=-s}^{s} \frac{2s+1}{s(s+1)} i^s \left\{ \operatorname{Re} \vec{\psi}^i_{2ts} \left[\delta_{t,1} + s(s+1) \delta_{t,-1} \right] \right.$$

$$\left. + \frac{1}{k_s} \operatorname{Re} \vec{\psi}^i_{3ts} \left[\delta_{t,1} - s(s+1) \delta_{t,-1} \right] \right\} \tag{8}$$

where δ_{mn} is the Kronecker δ. For the sake of simplicity, we write the incident wave field in terms of expansion co-efficients $a_{\tau n}$ as follows

$$\vec{u}^0 = \sum_{\tau n} a_{\tau n} \operatorname{Re} \vec{\psi}^i_{\tau n} e^{i k_\tau \cdot \vec{r}_i} \tag{9}$$

where $a_{\tau n}$ are the known incident field coefficients.

The unknown coefficients $b^i_{\tau n}$ can be related to $B^i_{\tau n}$ by means of any convenient scattering operator, in this case we employ the T-matrix, see Ref. [32].

$$B^i_{\tau n} = \sum_{\tau' n'} T^i_{\tau n, \tau' n'} b^i_{\tau' n'} . \tag{10}$$

Substituting Eqs. (6), (7) and (8) in (5), we obtain

$$\sum_{\tau n} b^i_{\tau n} \operatorname{Re} \vec{\psi}^i_{\tau n} = e^{i k_\tau \hat{z} \cdot \vec{r}_i} \sum_{\tau n} \operatorname{Re} \vec{\psi}^i_{\tau n} + \sum_{j \neq i}^{N} \sum_{\tau n} B^j_{\tau n} \vec{\psi}^j_{\tau n} \tag{11}$$

Since the field quantities are expanded with respect to centers of each scatterer, we obtain Eq. (9) with basis functions with respect to i-th and j-th centers. In order to express them with respect to a common origin 0_i, we employ the translation and addition theorems for the vector spherical functions [33] which may be written in a compact form as follows:

$$\vec{\psi}_{\tau n}^j = \vec{\psi}_{\tau n}(\vec{r}-\vec{r}_j) = \sum_{\tau'n'} \sigma_{\tau n \ \tau'n'} \ (\vec{r}_i-\vec{r}_j) \ \text{Re} \ \vec{\psi}_{\tau'n'}^i \quad . \tag{12}$$

Employing Eq. (12) in (11) and using the orthogonality of the vector spherical basis functions, we obtain the following set of coupled algebraic equations for the exciting field coefficients $b_{\tau n}^i$

$$b_{\tau n}^i = a_{\tau n} \ e^{i \ \vec{k}_\tau \cdot \vec{r}_i} + \sum_{j \neq i}^N \sum_{\tau'n'} B_{\tau'n'}^j \ \sigma_{\tau'n',\tau n} \ (\vec{r}_i-\vec{r}_j) \tag{13}$$

With the scattered field coefficients $B_{\tau n}^j$ expressed in terms of exciting field coefficients $b_{\tau n}^j$ and the T-matrix as given by (10), Eq. (13) gives the exciting field formulation of the multiple scattering. If we multiply both sides of Eq. (13) by the T-matrix, then we obtain the scattered field formulation of multiple scattering which may be written as

$$B_{\tau n}^i \equiv B_{\tau n}^{\ell(i)} = \sum_{\tau''n''} T_{\tau n, \tau''n''}^i \left[a_{\tau''n''} \ \exp(i \ \vec{k}_\tau \cdot \vec{r}) \right.$$

$$\left. + \sum_{j \neq i}^N \sum_{\tau'n'} B_{\tau'n'}^j \ \sigma_{\tau'n',\tau''n''} \ (\vec{r}_i-\vec{r}_j) \right] \quad . \tag{14}$$

From Eq. (14), it can be seen that the scattered field coefficients
of the i-th scatterer explicitly depend on the position and orientation
of other scatterers. In this paper, we consider a random distribution
of spherical scatterers and the case when $N \to \infty$ and the volume occupied
by the scatterers $V \to \infty$ such that $N/V = n_0$ is a finite number density.
For such distribution, a configurational average of Eq. (14) can be
made over the positions of all scatterers [28-32] with QCA [24] to arrive
at an equation for the configurational average $<B^i_{\tau n}>_i$ of the scattered
field coefficients with one scatterer fixed:

$$<B^i_{\tau n}>_i = \sum_{\tau''n''} T_{\tau n, \tau''n''} \left[a_{\tau''n''} e^{i \vec{k}_\tau \cdot \vec{r}_i} \right.$$

$$\left. + (N-1) \sum_{\tau'n'} \int_V p(\vec{r}_j|\vec{r}_i) <B^j_n>_j \sigma_{\tau'n' \ \tau''n''} d\vec{r}_j \right] \qquad (15)$$

where $p(\vec{r}_j|\vec{r}_i)$ is the two particle joint probability density.

The joint probability density is defined as

$$p(\vec{r}_j|\vec{r}_i) = \begin{cases} \frac{1}{V} g(|\vec{r}_j-\vec{r}_i|) & ; \quad |\vec{r}_j-\vec{r}_i| \geq 2a \\ \\ 0 & ; \quad |\vec{r}_j-\vec{r}_i| > 2a \end{cases}$$

Equation (16) implies that the particles are hard (no-interpenetration) and
the excluded volume is a sphere of radius 'a' although the particles
themselves may be non-spherical. The function $g(|\vec{r}_j-\vec{r}_i|)$ is
called the pair correlation function and depends only on $|\vec{r}_j-\vec{r}_i|$ due to

translational invariance of the system under consideration. The pair
correlation function for an ensemble of particles depends on the nature
and range of the interparticle forces. The average of several measurements
of a statistical variable that characterizes an ensemble will depend on
the pair correlation function. To obtain expressions for the pair
correlation function, one needs a description of the interparticle forces.
In our case we assume that the scatterers behave like effective hard
spheres (where the radius 'a' is that of the sphere circumscribing the
scatterer). Percus and Yevick [27] have obtained an approximate integral
equation for the pair correlation function of a classical fluid in
equilibrium. Wertheim [34] has obtained a series solution of the integral
equation for an ensemble of hard spheres. The statistics of the fluid
are then same as those of the ensemble of discrete hard particles that
we are considering.

Although integral expressions for the correlation functions also
result in a heirarchy, Percus and Yevick have truncated the heirarchy by
making certain approximations that result in a self-consistent relation
between the pair correlation function $g(x)$ and the direct correlation
function $C(x)$. The direct correlation function may be interpreted as
the correlation function resulting from an 'external potential' that
produces a simultaneous density fluctuation at a point and the external
potential is taken to be the potential seen by a particle given that
there is a particle fixed at another site. Fisher [35] comments that
the Percus-Yevick approximation is a strong statement of the extremely
short range nature of the direct correlation function. The integral
equation has the form

$$\tau(x) = 1 + n_o \int_{x<2a} \tau(x')dx' - n_o \int_{\substack{x'<2a \\ |x-x'|>2a}} \tau(x')\tau(x-x')dx' \qquad (17)$$

where

$$\begin{aligned}
\tau(x) &= g(x) & &; \ x > 2a \\
g(x) &= 0 & &; \ x < 2a \\
\tau(x) &= -C(x) & &; \ x < 2a \\
C(x) &= 0 & &; \ x > 2a
\end{aligned} \qquad (18)$$

Wertheim [34] has solved the integral equation by Laplace transformation that results in an analytic expression for $C(x)$ in the form

$$C(x) = -(1-n)^{-4} \left[(1+2n)^2 - 6n(1+\tfrac{1}{2}n)^2 x + n(1+2n)^2 x^3/2 \right] \ ; \ n = c/8 \qquad (19)$$

where 'c' is the effective spherical concentration of the particles. The Percus-Yevick approximation fails as the concentration approaches the close packing factor for spheres and is expected to be good for c < 0.3 or 0.4.

Equation (19) can be substituted back into Eq. (17) to yield a series solution for $g(x)$ in the form [34]

$$g(x) = \sum_{n=1}^{\infty} g_n(x) \qquad (20)$$

where

$$g_n(x) = \frac{1}{24nxi} \int e^{t(x-n)} \left[L(t) \mid S(t) \right]^n t\,dt \qquad (21)$$

where

$$S(t) = (1-n^2)t^3 + 6n(1-n)t^2 + 18n^2t - 12n(1+2n) \tag{22}$$

and

$$L(t) = 12\eta \left[(1+n2)t + (1+2n) \right] . \tag{23}$$

Throop and Bearman [36] have tabulated $g(x)$ as a function of x for values of $\eta = c/8$. A few representative plots of the pair correlation function are shown in Fig. 2.

To solve the integral equations given by (15), we consider the inhomogeneous medium with discrete scatterers as a homogeneous continuum and assume that the average coherent wave is a plane wave propagating with an effective wave number K in the same direction as the incident plane wave. We can thus write

$$<B^i_{\tau n}> = X_{\tau n} \, e^{i \vec{K} \cdot \vec{r}_i} \tag{24}$$

where $X_{\tau n}$ is the amplitude of the coherent wave.

Substituting Eq. (24) in (15) employing the joint probability function as defined before and the divergence theorem to convert the volume integral in (15) to surface integrals and using the extinction theorem which cancels the incident wave, we obtain a set of simultaneous coupled homogeneous equations for the coefficients $X_{\tau n}$ given by

$$X_{\tau n} = c \sum_{\tau''n''} \sum_{\tau'n'} \sum_{q=|n'-n''|}^{|n'+n''|} X_{\tau'n'} \, T_{\tau n, \tau''n''} \, C^q_{\tau'n', \tau''n''} \, \frac{I_q}{(k_\tau^2, -K^2)a^2} \tag{25}$$

where $c = 4\pi a^3 n_0/3$ is the effective spherical concentration of the scatterers per unit volume, C^q is an expression containing Wigner coefficients, and

$$I_q(K, k_\tau, c) = \frac{6c}{(k_\tau a)^2 - (Ka)^2} \; [2k_\tau a \; j_q(2Ka) \; h'_q(2k_\tau a)$$

$$-2Ka \; h_q(2k_\tau a) \; j_q(2Ka)] + 24c \int_{x=1}^{\infty} x^2 [g(x)-1] \; h_q(k_\tau x) \; j_q(Kx) \; dx \quad (26)$$

At low values of concentration c, $g(x) \approx 1$, see Fig. 2, and hence the integral in Eq. (26) is negligible which results in a system of uncorrelated hard particle statistics. This is what has been referred to as the 'well stirred approximation' (WSA) and yields the 'hole correction integral' as outlined by Fikioris and Waterman [37] and by us earlier. If $g(x) > 1$, one can regard the Eq. (26) as a modified 'hole correction integral' which is of the same form used by Twersky [26].

Equation (25) is a system of simultaneous linear homogeneous equations for the unknown amplitudes $X_{\tau n}$. For nontrivial solution, we require that the determinant of the truncated coefficient matrix vanishes, which yields an equation for the effective wave number K in terms of k_τ and the T-matrix of the scatterer. This is the dispersion relation for the scatterer filled medium. Equation (25) is a general expression valid for any arbitrary shaped scatterer, since the T-matrix is the only factor that contains information about the exact shape and boundary conditions at the scatterer. Thus the formalism presented here is valid for all the three wave fields. The effective wave number K obtained in the analysis is a

complex quantity, the real part of which relates to the phase velocity, while the imaginary part relates to attenuation of coherent waves in the medium.

Results and Conclusions

In the Rayleigh or low frequency limit, the size of the scatterers is considered to be small when compared to the incident wavelength. It is then sufficient to take only the lowest order coefficient in the expansion of the fields. In this limit, the elements of the T-matrix can be obtained in closed form for various simple shapes (46). It can be shown that at low frequencies, only $X_{\tau 0}$, $X_{\tau 1}$ and $X_{\tau, -1}$ of Eq. (25) make a contribution. After some manipulations of the resulting 3 x 3 determinant, we obtain the following dispersion relations for elastic spherical inclusions embedded in a different elastic medium (matrix):

$$\left(\frac{k_p}{k_s}\right)^2 = \frac{(1+9c\ E_1)(1+3c\ E_0)\left[\ 1+3c\ \frac{E_2}{2}\ (2+\frac{3k_s^{\ 2}}{k_p^{\ 2}}\ )\right]}{1-15c\ E_2\left[1+3c\ E_0\right]+\frac{3}{2}\ c\ E_2\left(2+\frac{3k_s^{\ 2}}{k_p^{\ 2}}\right)} \tag{27}$$

$$\left(\frac{k_s}{k_s}\right)^2 = \frac{(1+9c\ E_1)\left(1+\frac{3}{2}\ c\ E_2\left[2+\frac{3k_s^{\ 2}}{k_p^{\ 2}}\right]\right)}{1+\frac{3}{4}\ c\ E_2(4-\frac{9k_s^{\ 2}}{k_p^{\ 2}}\ )} \tag{28}$$

where

$$E_0 = \frac{1}{3} \frac{3\lambda + 2\mu - (3\lambda_1 + 2\mu_1)}{4\mu + 3\lambda_1 + 2\mu_1}$$

$$E_1 = \frac{1}{9} \left(\frac{\rho_1}{\rho} - 1\right)$$

(29)

$$E_2 = -\frac{\frac{4}{3} \mu(\mu_1 - \mu) \ 24\mu_1(\mu_1 - \mu) - (\lambda_1 + 2\mu_1)(19\mu_1 + 16\mu)}{24\mu_1(\mu_1 - \mu) - (\lambda_1 + 2\mu_1)(19\mu_1 + 16\mu) \ .}$$

$$\times \frac{1}{4\mu(\mu_1 - \mu) + 3(\lambda + 2\mu)(2\mu_1 + 3\mu)}$$

and $c = 4\pi a^3 n_0/3$ is the concentration of spheres, and K_p and K_s are the coherent wave numbers for longitudinal and shear waves, respectively, in the new medium. Similar expressions can also be derived for spheroidal inclusions using the T-matrix obtained in Refs. [32,38]. In the Rayleigh limit, the value of K as determined by the above dispersion relations is a real quantity for lossless (elastic) material and a complex quantity for lossy (viscoelastic) material, and relates to phase velocity $V_p = \omega/K$. In this limit, we normally study the dependence of phase velocity on concentration, angle of incidence and aspect ratio of the scatterers. The teneral tendency of the phase velocity is to increase slightly (for inclusion) and decrease slightly (for cracks and cavities) as concentration increases. Thus, the phase velocity vs. concentration information is not very useful both from theoretical and experimental point of view. The

plots of absorption and coherent attenuation due to multiple scattering vs. frequency for various concentrations carry more information which may eventually be used for designing absorbing materials [39].

The dispersion relations given in Eqs. (27) and (28) may also be useful in obtaining the effective shear modulus and bulk modulus at low frequencies. Following the work by us [20,22] and by Bedeaux and Mazur [21], we arrive at the following shear and bulk moduli ($<\mu>$ and $<B>$) of an elastic material containing a random distribution of stress free bubbles or cavities

$$\frac{<\mu>}{\mu} = \frac{4\mu - 3c \ E_2 \ (9\lambda + 14\mu)}{4\mu + 6c \ E_2 \ (3\lambda + 8\mu)} \tag{30}$$

$$\frac{<B>}{B} = \frac{3\lambda + 2\mu \ [1 - 6c \ E_0]}{(3\lambda + 2\mu) \ [1 + 3c \ E_0]} \tag{31}$$

where E_0 and E_2 are defined in Eq. (29).

To study the response at resonant and higher frequencies, we must consider higher powers of $k_\tau a$, and this implies that a larger number of terms ($X_{\tau n}$) must be kept in the expansion of the average field. This is best done numerically. For a given value of ka, the T-matrix for the scatterer is computed. Next, the coefficient matrix M corresponding to $X_{\tau n}$ (Eq. (25) is formed. The complex determinant of the coefficient matrix is computed using standard Gauss elimination techniques. For a given $k_\tau a$, the root of the equation det M = 0 is searched in the complex K plane ($K_1 + iK_2$) using Muller's method. Good initial guesses were provided by the Rayleigh limit solutions at low values of $k_\tau a$ and

these could be used systematically to obtain convergence of roots at increasingly higher values of $k_\tau a$. The real part K_1 determines the phase velocity, while the imaginary part K_2 determines the coherent wave attenuation.

Here, we present some sample numerical calculation of spherical glass inclusion in epoxy matrix. The longitudinal and shear wave velocities of the glass and epoxy matrix are taken as $(c_p)_1$ = 5.28 mm/μsec, c_p = 2.54 mm/μsec, $(c_s)_1$ = 3.24 mm/μsec and c_s = 1.16 mm/μsec, respectively. We consider a concentration of 44.1% to reflect a high concentration. The coherent wave attenuation vs. frequency (longitudinal wave number) for this configuration is shown in Fig. 3. The general tendency of attenuation is to increase at lower frequencies and shows some oscillation as shown. These results are compared with some experimental observations for the same composite obtained by Kinra (private communication). The theoretical results obtained in this paper compare with Kinra's experimental results qualitatively not quantitatively. The reason for this factor difference must be explored in the future. The oscillation at higher frequencies, however, indicate that the scattering is mostly in the forward direction. Thus, in this case repeated scattering should not be important, since the backscattered wave is significantly smaller than the forward scattered wave. The same observation may be noticed even for electromagnetic waves [28] where the theoretical results obtained by our theory are compared with experimental data. (The paper [28] is enclosed for the benefit of the reader.

Since the phase velocity does vary very slightly as a function of frequency, the bulk properties depend totally on coherent wave attenuation

only.   Thus, one can compute the bulk properties which can be plotted
in the complex plane (Cole-Cole plot) as shown in our paper [30] which
is also enclosed.

Recommendations for Future Work

It is obvious from the preceding discussions on the QCA as well as
the numerical results that the two major improvements required are for
the QCA as well as the pair correlation function, so that good results
can be obtained for all concentrations even at long and intermediate
values of the wavelength.   In a review article, Lax [40] has suggested
that in the quantum mechanical context, the QCA could be improved by
using modified propagators for the fields.   In the classical context,
this implies that on the average, single particle scattering takes place
in a macroscopically homogeneous medium, and, in this respect, this idea
is the same as the coherent potential approximation (CPA) of Solid State
Physics.   The repeated multiple scattering between pairs of scatterers
or cluster effects can be improved by making the self consistent
approximation (SCA) in addition to the CPA.

For the purpose of discussion of these ideas within the T-matrix
formalism given earlier, we denote by $\vec{u}_j^s$ and $\vec{u}_j^e$ the fields scattered by
and exciting the j-th scatterer, respectively.   The expansion coefficients
of these fields are denoted by B^j and b^j, respectively, omitting all
subscripts.

The CPA can be expressed succinctly as

$$<B^j>_j = T(K) <b^j>_j \tag{32}$$

where the T-matrix relating the exciting and scattered field coefficients is evaluated using the bulk propagation constant K for the embedding medium. Thus the CPA implies that the field scattered by a single obstacle in the presence of several others when averaged over the position of all scatterers is the same as the field that would be produced by a single particle embedded in a macroscopically homogeneous medium described by the propagation constant K. The incorporation of the CPA into the previous formalism involves changes only in the computations and a redefinition of the T-matrix in Eq. (10). It would be interesting to see the change, if any, in the numerical computations as a result of invoking the CPA.

The idea behind the 'self consistent approximation' (SCA) is somewhat more suble. From the discussion in the section on the QCA, it is now clear that QCA-CPA neglects multiple scattering between two fixed scatterers. The SCA as defined by Schwartz and Ehrenreich [41] restores this by stating that

$$<B^j>_{ij} = T(K) <b^j>_j \tag{33}$$

where T(K) is the T-matrix of scatterer 'j' in the presence of scatterer 'i' in the effective medium with propagation constant K. Expressions for T(K) as given by Varadan and Varadan [42] may be written as

$$T(K) = R(\vec{r}_{ij}/2) \quad T[1-\sigma(-\vec{r}_{ij})T\sigma(r_{ij})T]^{-1}$$

$$[1+\sigma(-\vec{r}_{ij})TR(\vec{r}_{ij})] \quad R(-\vec{r}_{ij}/2) \tag{34}$$

where σ is a compact notation for the translation matrices B and C introduced in Eq. (12). The R matrix is simply the part of σ that is regular at the origin, i.e., for $|\vec{r}_{ij}| = 0$. All matrices in Eq. (34) are obtained using the bulk Propagation Constant for the host medium.

We observe that $T(K)$ explicitly depends on r_{ij} the distance between 'i' and 'j'. The integration procedure will no longer be simple as before and the SCA may be rather difficult to enforce in computations, especially if more realistic models are chosen for the pair correlation function.

Incorporation of the CPA as well as improved models of the pair correlation function into our computations are in progress. We hope that they will shed some light on the sensitivity of multiple scattering theories to approximations like QCA and SCA as a function of frequency and scatterer concentration. Needless to say additional experimental results are required for comparison with these computations.

Acknowledgments

References

1. P.C. Waterman and R. Truell, "Multiple Scattering of Waves," _J. Math. Phys._, 2, 512 (1961).

2. V.M. Merkulova, "Acoustical Properties of Some Solid Hetrogeneous Media at Ultrasonic Frequencies," _Sov. Phys. Acoust._, 11, 55 (1965).

3. I.A. Chaban, "Self-Consistent Field Approach to Calculation of the Effective Parameters of Microinhomogeneous Media," _Sov. Phys. Acoust._, 10, 298 (1964).

4. I.A. Chaban, "Calculation of the Effective Parameters of Micro-inhomogeneous Media by the Self-Consistent Field Method," _Sov. Phys. Acoust._, 11, 81 (1965).

5. A.K. Chatterjee and A.K. Mal, "Elastic Moduli of Two-Component Systems," _J. Geophys. Res._, 83, 1785 (1978).

6. E. Domany, J.E. Gubernatis and J.A. Krumhansl, "The Elasticity of Polycrystals and Rocks," _Materials Science Center Report_, Cornell University, New York (1974).

7. J. Korringa, "Theory of Elastic Constants of Heterogeneous Media," _J. Math. Phys._, 4, 509 (1973).

8. E. Kröner, "Elastic Moduli of Perfectly Disordered Composite Materials," _J. Mech. Phys. Solids_, 15, 319 (1967).

9. S.K. Datta, "Scattering of a Random Distribution of Inclusions and Effective Elastic Properties," in the _Proceedings of Continuum Models of Discrete Systems_, University of Waterloo (1977).

10. V.K. Varadan, V.V. Varadan and Y.H. Pao, "Multiple Scattering of Elastic Waves by Cylinders of Arbitrary Cross Section - I. SH-Waves," _J. Acoust. Soc. America_, 63, 1310 (1978).

11. V.K. Varadan and V.V. Varadan, "Frequency Dependence of Elastic (SH-) Wave Velocity and Attenuation in Anisotropic Two Phase Media," _Int. J. Wave Motion_, 1, 53 (1979).

12. V.K. Varadan, "Scattering of Elastic Waves by Randomly Distributed and Oriented Scatterers," _J. Acoust. Soc. America_, 65, 655 (1979).

13. V.K. Varadan and V.V. Varadan, "Multiple Scattering of Elastic Waves by Cylinders of Arbitrary Cross Section II -P and SV Waves," _Materials Science Center Report_, #2937, Cornell University, New York (1977).

14. V.K. Varadan, "Dispersion of Longitudinal Shear Waves in a Medium Containing Periodic Arrays of Cylinders of Arbitrary Cross Section," Proceedings of the 14th Annual Meeting of the Society of Engineering Science, Lehigh University, Pennsylvania (1977).

15. V.K. Varadan and V.V. Varadan, "Dynamic Elastic Properties of a Medium Containing a Random Distribution of Obstacles - Scattering Matrix Theory," Material Science Center Report #2740, Cornell University, New York (1976).

16. V.K. Varadan, V.V. Varadan, V.N. Bringi and T.A. Seliga, "Acoustics, Electromagnetic and Elastic Wave Fields," Proceedings of International IEEE/AP-S Symposium USNC/URSI Meeting, University of Colorado, Boulder, Colorado (1978).

17. V.K. Varadan, V.N. Bringi and V.V. Varadan, "Coherent Electromagnetic Wave Propagation Through Randomly Distributed Dielectric Scatterers," Phy. Rev. D., 19, 2480 (1979).

18. V.V. Varadan and V.K. Varadan, "Multiple Scattering of Electromagnetic Waves by Randomly Distributed and Oriented Dielectric Scatterers," Phys. Rev. D., 21, 388 (1980).

19. V.K. Varadan, "Multiple Scattering of Acoustic, Electromagnetic and Elastic Waves," in Acoustic, Electromagnetic and Elastic Wave Scattering-Focus on the T-matrix Approach (Edited by V.K. Varadan and V.V. Varadan), Pergamon Press, New York (1980).

20. V.K. Varadan and V.V. Varadan, "Characterization of Dynamic Shear Modulus in Inhomogeneous Media Using Ultrasonic Waves," First International Symposium on Ultrasonic Materials Characterization, NBS, June (1978).

21. D. Bedeaux and P. Mazur, "On the Critical Behavior of the Dielectric Constant for a Nonpolar Fluid," Physica, 67, 23 (1973).

22. V. Varatharajulu (V.V. Varadan) and D.J. Vezzetti, "Approach of the Statistical Theory of Light Scattering to the Phenomenological Theory," J. Math. Phys., 17, 232 (1976).

23. L.L. Foldy, "The Multiple Scattering of Waves I. General Theory of Isotropic Scattering by Randomly Distributed Scatterers," Phys. Rev. 67, 107 (1945).

24. M. Lax, "Multiple Scattering of Waves II. Effective Field in Dense Systems," Phys. Rev., 85, 621 (1952).

25. A.K. Mal and S.K. Bose, "Dynamic Elastic Moduli of a Suspension of Imperfectly Bonded Spheres," Proc. Camb. Phil. Soc., 76, 587 (1974).

26. V. Twersky, "Coherent Electromagnetic Waves in Pair-Correlated Random Distribution of Aligned Scatterers," J. Math. Phys., 19, 215 (1979).

27. J.K. Percus and G.J. Yevick," Analysis of Classical Statistical Mechanics by Means of Collective Coordinates," Phys. Rev., 110, 1 (1958).

28. V.N. Bringi, T.A. Seliga, V.K. Varadan, V.V. Varadan, "Bulk Propagation Characteristics of Discrete Random Media," in Multiple Scattering and Waves in Random Media (Edited by P.L. Chow, W.E. Kohler and G.C. Papanicolaou), North-Holland Publishing Company, Amsterdam, 43 (1981).

29. V.N. Bringi, V.V. Varadan and V.K. Varadan, "The Effects of Pair Correlation Function on Coherent Wave Attenuation in Discrete Random Media," IEEE Antennas and Propagation, in press.

30. V.V. Varadan, V.N. Bringi and V.K. Varadan, "Frequency Dependent Dielectric Constants of Discrete Random Media," The Ohio State University Research Foundation Report, 1981.

31. V.V. Varadan, V.N. Bringi, T.A. Seliga and V.K. Varadan, "Coherent Wave Attenuation by a Random Distribution of Particles," J. Radio Science, invited paper (to be published in 1982).

32. V.K. Varadan and V.V. Varadan (Eds.) Acoustic, Electromagnetic and Elastic Wave Scattering - Focus on the T-matrix Approach, Pergamon Press, New York (1980).

33. A. Boström, "Multiple Scattering of Elastic Waves by Bounded Obstacles," J. Acoust. Soc. Am., 67, 399 (1980).

34. M.S. Wertheim, "Exact Solution of the Percus-Yevick Integral Equation for Hard Spheres," Phys. Rev. Lett., 10, 321 (1963).

35. I.Z. Fisher, Statistical Theory of Liquids, The University of Chicago Press, Chicago, 309 (1965).

36. G.J. Throop and R.J. Bearman, "Numerical Solutions of the Percus-Yevick Equation for the Hard-sphere potential," J. Chem. Phys. 42, 2408 (1965).

37. J.G. Fikioris and P.C. Waterman, "Multiple Scattering of Waves II. Hole Corrections in the Scalar Case," J. Math. Phys. 5, 1413 (1964).

38. V.V. Varadan and V.K. Varadan, "Low Frequency Expressions for Acoustic Wave Scattering Using Waterman's T-matrix Method," J. Acoust. Soc. Am. 66, 586 (1979).

39. R.D. Corsaro and J.D. Klunder, "A Filled Silicone Rubber Materials System with Selectable Acoustic Properties for Molding and Coating Applications at Ultrasonic Frequencies," Naval Research Laboratory Report #8301, May 11 (1979).

40. M. Lax, "Wave Propagation and Conductivity in Random Media," in Stochastic Differential Equations (SIAM-AMS Proceedings, VI, 1973).

41. L. Schwartz and H. Ehrenreich, "Single Site Approximations in the Electronic Theory of Liquid Metals," Ann. Phys. 64, 100 (1971).

42. V.V. Varadan and V.K. Varadan, "Configurations with Finite Numbers of Scatterers - A Self-Consistent T-matrix Approach," J. Acoust. Soc. Am., 70, 213 (1981).

39. R.D. Corsaro and J.D. Klunder, "A Filled Silicone Rubber Materials System with Selectable Acoustic Properties for Molding and Coating Applications at Ultrasonic Frequencies," <u>Naval Research Laboratory Report #8301</u>, May 11 (1979).

40. M. Lax, "Wave Propagation and Conductivity in Random Media," in Stochastic Differential Equations (SIAM-AMS Proceedings, VI, 1973).

41. L. Schwartz and H. Ehrenreich, "Single Site Approximations in the Electronic Theory of Liquid Metals," <u>Ann. Phys.</u> 64, 100 (1971).

42. V.V. Varadan and V.K. Varadan, "Configurations with Finite Numbers of Scatterers - A Self-Consistent T-matrix Approach," <u>J. Acoust. Soc. Am.</u>, 70, 213 (1981).
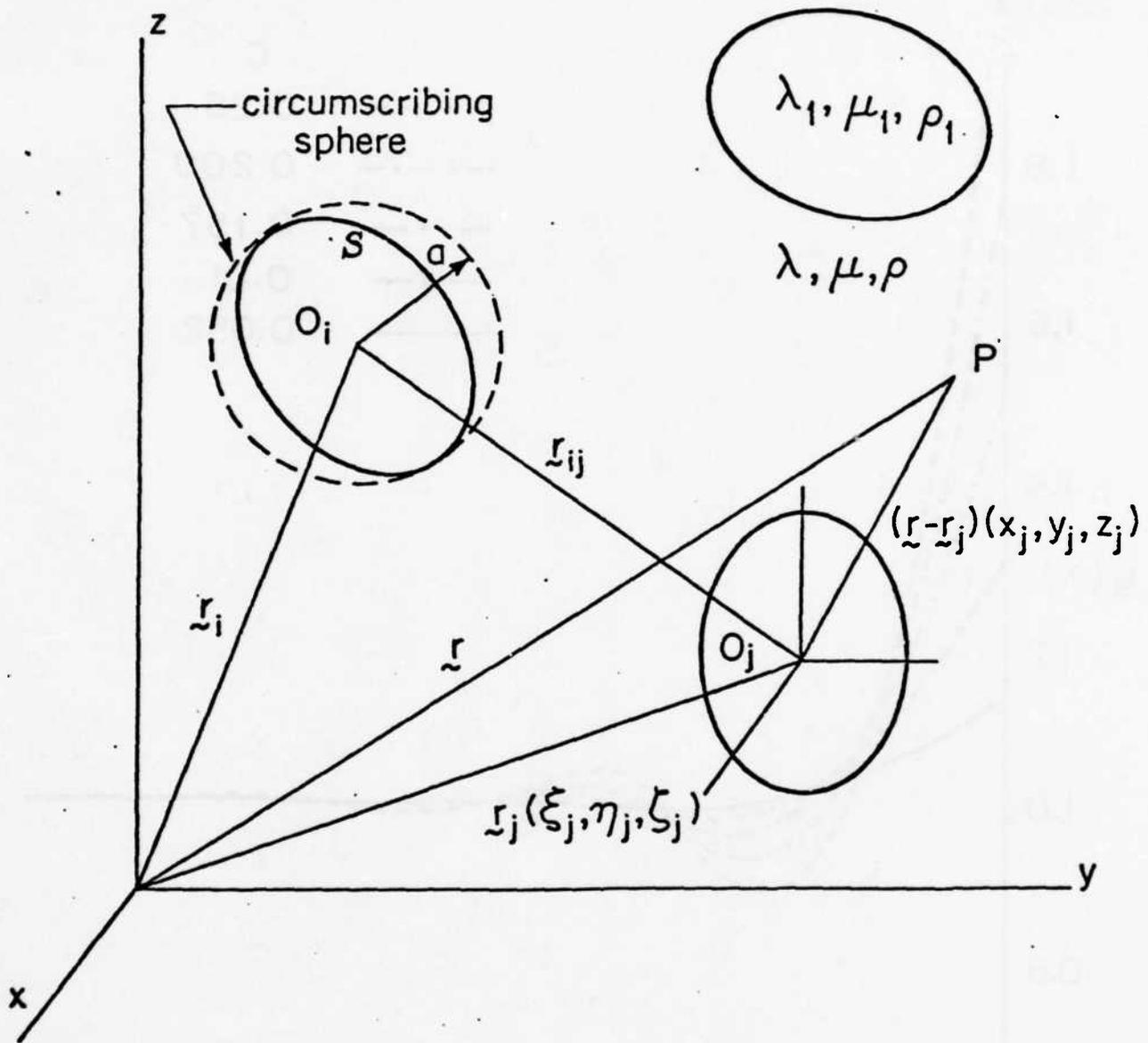
Figure 1. Random distribution of inclusions of arbitrary shape
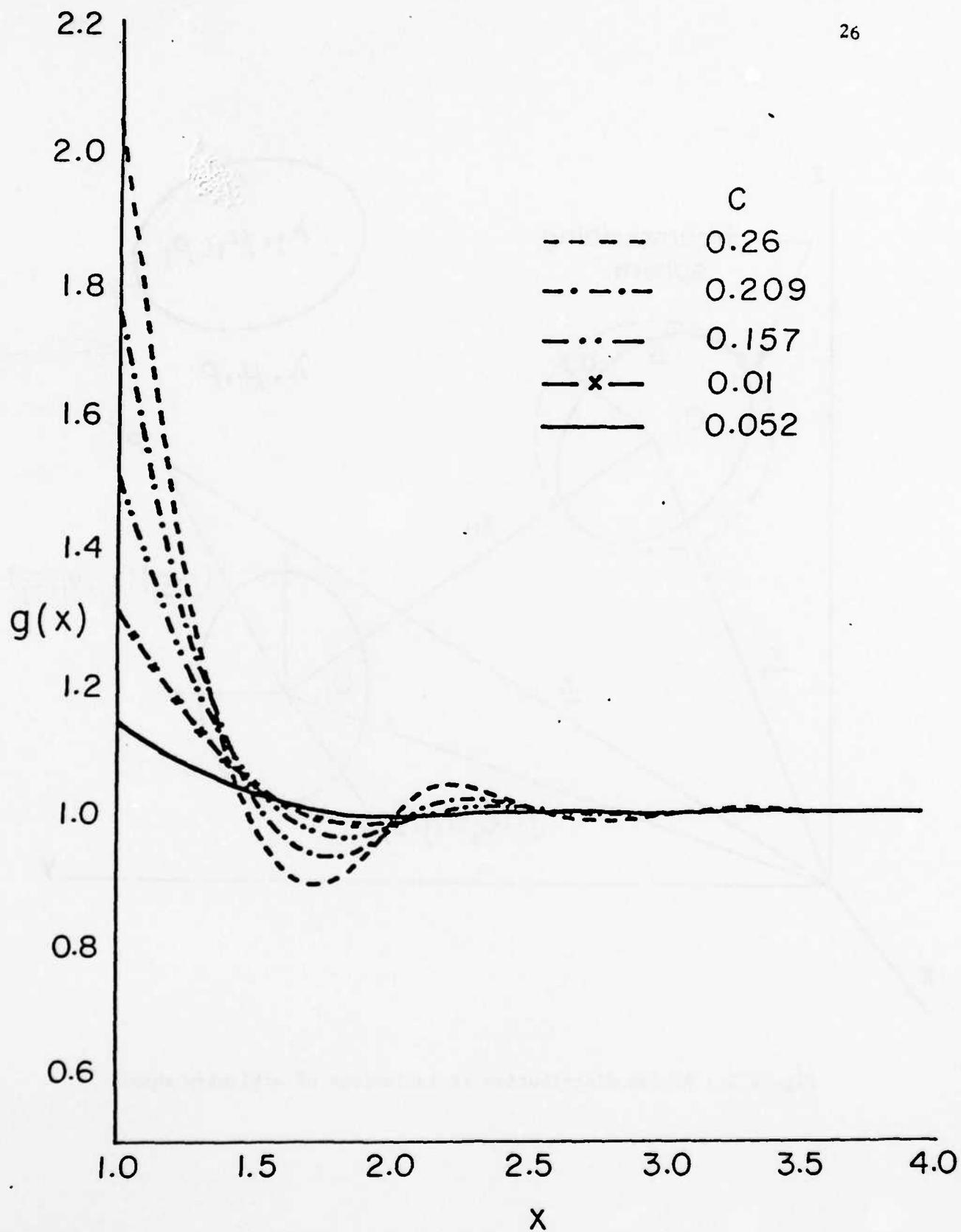
Figure 2. The Percus-Yevick pair correlation function for hard spheres as given by Throop and Bearman (1964)
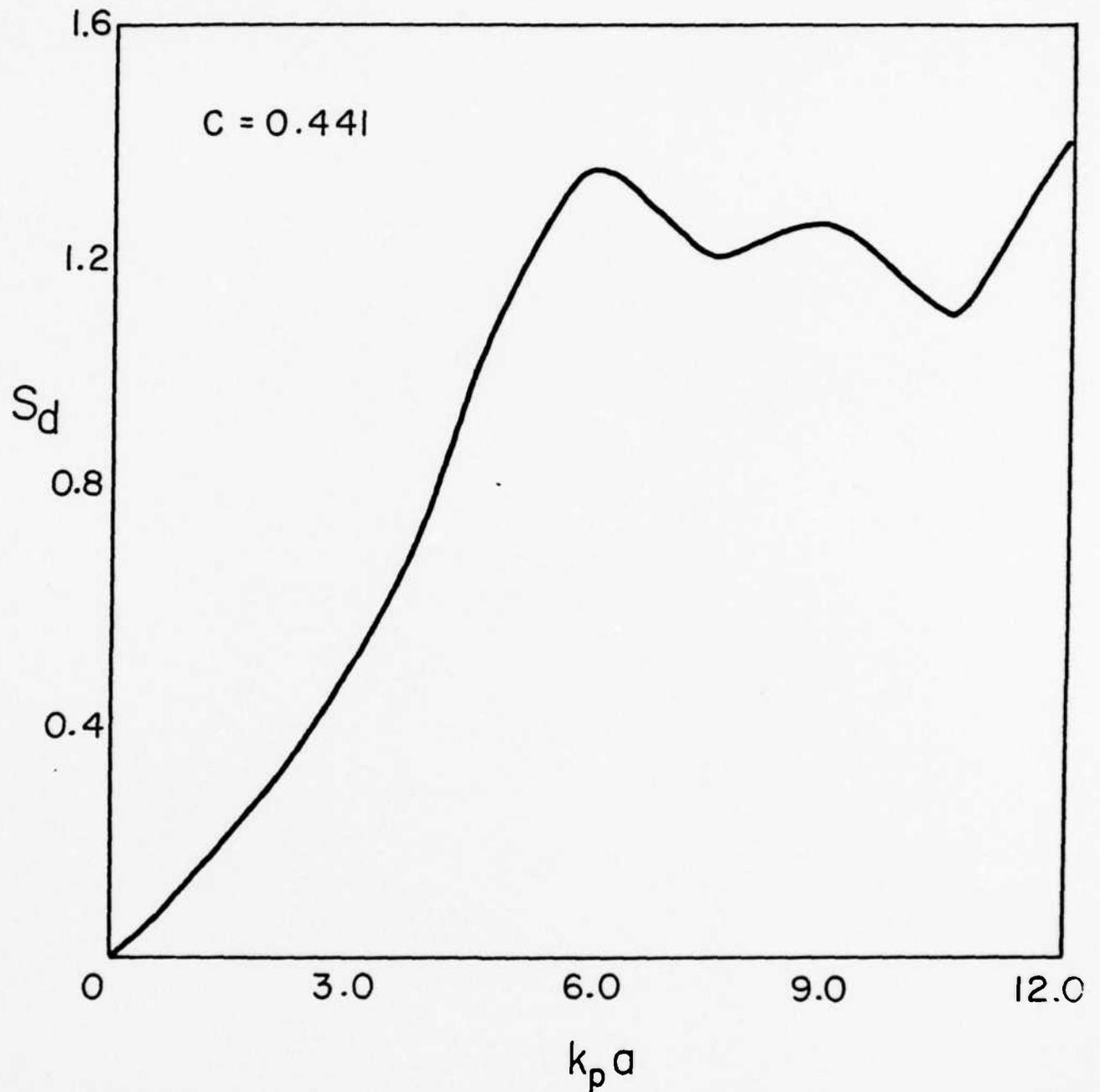
Figure 3. The coherent attenuation $S_d = 4\pi \ Im(K_\tau/k_\tau)$ vs $k_p a$ for glass spheres in epoxy matrix

COMPARISON OF SOUND SCATTERING BY
RIGID AND ELASTIC OBSTACLES IN WATER

by

V.K. Varadan, V.V. Varadan, J.H. Su and T.A.K. Pillai
Wave Propagation Group
Department of Engineering Mechanics
The Ohio State University
Columbus, Ohio 43210

ABSTRACT

Acoustic wave scattering by prolate and oblate spheroids and finite
cylinders immersed in water is compared when rigid body and elastic
boundary conditions respectively are satisfied at the fluid-scatterer
interface. The results obtained in the case of rigid body boundary
conditions are new. The frequency dependence of the scattered far field
is obtained for various angles of incidence for both types of boundary
conditions using the Null Field or T-matrix approach. From our computations
it is concluded that only for restricted material properties of the
scatterer, scattering geometry and scatterer shape, the scattering
characteristics of an elastic obstacle and a rigid obstacle of the same
shape are comparable up to wavelengths comparable to the size of the
obstacle.

INTRODUCTION

For submerged obstacles in water where rigid boundary conditions are rarely satisfied, it has been demonstrated by some authors[1-3] that the scattering of solid elastic obstacle, whose density and wave velocity is much higher than that of water, closely follows the corresponding results for a rigid body until the lowest order resonance due to the excitation of a Rayleigh surface wave is observed[2,4,5]. The results are thus usually interpreted in terms of a rigid body reflection term and a resonance term. This is particularly true for a material such as tungsten carbide[6]. Other important considerations are the geometry of the obstacle and the angle of the incident wave in question. Until a few years ago, numerical results were available only for infinite circular cylinders and spheres especially for the elastic case.

The purpose of this paper is to compare the scattering of acoustic waves by non-spherical rigid and elastic obstacles immersed in water so that one can verify if in fact the scattered pressure field produced by rigid and elastic obstacles of the same shape are the same for a wide range of frequencies of the incident plane wave, as well as several angles of incidence. The geometries that we consider are the prolate spheroid, the oblate spheroid and a finite circular cylinder with hemispherical end caps. The first two represent quite well long, narrow and flat obstacles respectively while the third is a good practical model to test the effectiveness of the scattering theory proposed here.

Recently, theoretical results have been obtained for the elastic obstacle in water for all three cases[7-9] using the Null field or T-matrix

method for arbitrary angle of incidence. For a review of the T-matrix approach, we refer to Varadan and Varadan[10]. Surprisingly enough results are not presently available in the literature for the scattering of sound waves by rigid scatterers although this is easier than the corresponding problem with an elastic obstacle. At the present time the only result that can be found in the literature for non-spherical rigid scatterers are those given by Bowman, Senior and Uslenghi[11-13]. They have presented the frequency dependence of the scattering cross section of several different prolate and oblate spheroids but with the restriction that the incident plane wave propagates along the symmetry axis of the spheroid. The method employed by them is the separation of variables approach employing spheroidal functions. It is generally understood that spheroidal functions of non-zero azimuthal index are difficult to compute numerically and these are necessary to study the case of oblique incidence. Moreover, numerical results are not available for rigid finite cylinders in the literature. Experimental investigations in the high frequency range have been carried out by Dragonette[13], Lang[14] et. al, for various rigid non-spherical scatterers and comparisons were made with the modified Freedman theory[15].

In Section II, the necessary equations for obtaining the T-matrix of a rigid scatterer are presented briefly. Details of the formulation may be obtained from Refs. 8 and 4. In Section III, numerical results are presented for rigid prolate and oblate spheroids as well as finite circular cylinders with spherical end caps. These results are presented in terms of the far field scattered pressure as a function of frequency for several scattering geometries. Comparisons are made with the corresponding case of elastic obstacles and the similarities and

2

differences are noted and discussed. From our computations it is concluded that only for restricted material properties of the scatterer, scattering geometry and scatterer shape, and the scattering characteristics of an elastic obstacle and a rigid obstacle of the same shape are comparable up to wavelengths comparable to the size of the obstacle.

II. T-MATRIX OF RIGID AND ELASTIC OBJECTS IN WATER

a) Rigid Objects

Consider an obstacle described by the boundary S and continously turning unit outward normal $\hat{n}$ immersed in a fluid of mass density ρ_f and compressibility λ_f. A plane harmonic wave of frequency ω is incident on the scatterer. All fields will have the same harmonic time dependence and this time dependence is not written explicitly. The pressure ϕ in the fluid is given by

$$\phi(\vec{r}) = \phi^o(\vec{r}) + \phi^S(\vec{r}) \quad ; \quad \vec{r} \text{ outside } S \tag{1}$$

where ϕ^o and ϕ^S are the incident and scattered pressure fields respectively. All three fields satisfy the Helmholtz equation given by

$$\left(\nabla^2 + \frac{\omega^2}{c_f^2} \right) \begin{pmatrix} \phi \\ \phi^o \\ \phi^S \end{pmatrix} = 0 \tag{2}$$

where c_f is the sound speed in the fluid. The integral representation and the extended boundary condition or null field equation have been presented in Waterman's original paper on the T-matrix formulation of acoustic wave scattering[16]. They are

$$\int_S \left\{ \phi_+ \ \hat{n} \cdot \nabla' g(\vec{r}, \vec{r}') - (\hat{n} \cdot \nabla'_+ \phi) \ g(\vec{r}, \vec{r}') \right\} dS$$

$$= \begin{cases} \phi^S(\vec{r}) & ; \ \vec{r} \text{ outside } S \\ -\phi^o(\vec{r}) & ; \ \vec{r} \text{ inside } S \end{cases} \tag{3}$$

4

where

$$g(\vec{r}, \vec{r}') = \exp \left[i \, k_f |\vec{r} - \vec{r}'| \right] / \, k_f |\vec{r} - \vec{r}'| \quad ; \quad k_f = \omega/c_f \qquad (4)$$

is the free space Green's function of the Helmholtz equation. The quantities ϕ_+ and $\hat{n} \cdot \nabla'_+ \phi$ are respectively the pressure and normal component of the fluid velocity just on the outside of S.

If the scatterer is rigid, the boundary condition at S is that

$$\hat{n} \cdot \nabla'_+ \phi(\vec{r}') = 0 \quad ; \quad \vec{r}' \text{ on S} \qquad (5)$$

The philosophy of the T-matrix approach is to expand all field quantities appearing in Eq. (3) in terms of a set of spherical functions in order to obtain the T-matrix that relates the known coefficients of expansion of the incident plane harmonic wave to the unknown expansion coefficients of the scattered field. To this end we define the following scalar basis function

$$\phi_{fnm\sigma}(\vec{r}) = \xi_{nm} \, h_n(k_f r) \, P_n^m(\cos \theta) \begin{pmatrix} \cos m\phi \quad ; \quad \sigma = 1 \\ \\ \sin m\phi \quad ; \quad \sigma = 2 \end{pmatrix} \qquad (6)$$

where

$$\xi_{nm} = \left[\epsilon_m \, \frac{(2n+1) \, (n-m)!}{4\pi \, (n+m)!} \right]^{1/2} \quad ; \quad \epsilon_o = 1, \, \epsilon_m = 2 \; ; \; n > 0.$$

The wave function defined above may be used to expand fields that satisfy radiation conditions at infinity, but to expand fields that are finite at the origin, we replace the Hankel function $h_n(\cdot)$ by the spherical

5

Bessel functions $j_n(\cdot)$. The functions that are regular at the origin are denoted by the letter 'Re'. Here 'Re' stands for regular rather than real.

The incident and scattered fields outside S are expanded according to

$$\phi^o(\vec{r}) = \sum_{n=0}^{\infty} \sum_{m=0}^{\infty} \sum_{\sigma=1}^{2} a_{nm\sigma} \text{ Re } \phi_{fnm\sigma}(\vec{r}) \tag{7}$$

$$\phi^S(\vec{r}) = \sum_{n=0}^{\infty} \sum_{m=0}^{\infty} \sum_{\sigma=1}^{2} f_{nm\sigma} \phi_{fnm\sigma}(\vec{r}) \tag{8}$$

where $a_{nm\sigma}$ are known and $f_{nm\sigma}$ are unknown. For a plane harmonic wave incident in the x-z plane ($\phi_o = 0$), see Fig. 2

$$a_{nm\sigma} = \frac{4\pi}{k_f} \xi_{nm} i^{n-1} P_n^m(\theta_o) \delta_{\sigma,1} \tag{9}$$

The Green's function g and the unknown surface pressure ϕ_+ in Eq. (3) are also expanded as follows:

$$g(\vec{r},\vec{r}') = i k_f \sum_n \sum_m \sum_\sigma \phi_{fnm\sigma}(r_>) \text{ Re } \phi_{fnm\sigma}(r_<), \tag{10}$$

$$\phi_+(\vec{r}) = \sum_n \sum_m \sum_\sigma \alpha_{nm\sigma} \phi_{fnm\sigma}(\vec{r}) \tag{11}$$

Using Eqs. (5) - (11) in Eq. (3) and considering points $\vec{r}$ that are inside the sphere inscribing S and points $\vec{r}$ that are outside the sphere circumscribing S respectively (see Fig. 1) we obtain [16]

6

$$i \sum_{n'} \sum_{m'} \sum_{\sigma'} Q_{nm\sigma,n'm'\sigma'} \, \alpha_{n'm'\sigma'} = -a_{nm\sigma} \tag{12}$$

and

$$i \sum_{n'} \sum_{m'} \sum_{\sigma'} \text{Re} \, Q_{nm\sigma,n'm'\sigma'} \, \alpha_{n'm'\sigma'} = f_{nm\sigma} \tag{13}$$

where

$$Q_{nm\sigma,n'm'\sigma'} = \int_S \text{Re} \, \phi_{fn'm'\sigma} \, \hat{n} \cdot \nabla \, \phi_{fnm\sigma} \, dS \tag{14}$$

From Eqs. (12) and (13), we obtain the following relationship between the incident and scattered field coefficients

$$f = -Ta \tag{15}$$

where T is the T-matrix given by

$$T_{nm\sigma,n'm'\sigma'} = \sum_{n''m''\sigma''} \text{Re} \, Q_{nm\sigma,n''m''\sigma''} \, Q^{-1}_{n''m''\sigma'',n'm'\sigma'} \tag{16}$$

The T-matrix depends on the frequency of the incident wave, the geometry of the obstacle and the boundary conditions at the interface.

Any symmetries that the scatterer has will reduce certain elements of the T- and Q-matrices to zero. Scatterers with an axis of revolution will make the Q- and T-matrices block diagonal in the azimuthal index thus simplifying the computations.

From Eqs. (15) and (16), we obtain expressions for the coefficients of expansion of the scattered field. At distances far from S, the field

7

consists of outgoing spherical waves with an amplitude that depends on θ and ϕ. The amplitude of the scattered far field may be written as

$$f(\theta,\phi) = \sum_n \sum_m \xi_{nm} \, i^{-n} \, P_n^m(\cos \theta) \, [f_{1mn}\cos m\phi + f_{2mn}\sin m\phi] \qquad (17)$$

where we have explicitly written all subscripts and superscripts for the scattered field coefficients $f_{nm\sigma}$.

b) Elastic Obstacle

Now we consider an elastic scatterer of arbitrary surface S immersed in water. The elastic properties of the scatterer are given by the Lamé constants λ and μ and mass density ρ while the properties of the fluid are given by the compressibility λ_f and mass density ρ_f. In this case although the scatterer is again immersed in a fluid governed by the scalar wave equation, it is convenient to use a vector formalism for both the fluid (outside S) and solid (inside S) regions to facilitate application of the boundary conditions. All the details of the vector formulation have been given in Ref. 2. Only the most pertinent results will be presented here.

The integral representation for the displacement field $\vec{u} = \vec{u}^o + \vec{u}^S$, the sum of the incident and scattered parts, in the fluid region is given by

$$\int_S \left\{ u'_+ \cdot [\hat{n}' \cdot \overset{\leftrightarrow}{\Sigma}_f(\vec{r},\vec{r}')] - \overset{\leftrightarrow}{G}_f(\vec{r},\vec{r}') \cdot \vec{t}'_+ \right\} dS'$$

$$= \begin{cases} \vec{u}^S & ; \quad \vec{r} \text{ outside S} \\ -\vec{u}^o & ; \quad \vec{r} \text{ inside S} \end{cases} \tag{18}$$

where $\overset{\leftrightarrow}{G}_f$ and $\overset{\leftrightarrow}{\Sigma}_f$ are the vector analogs of the free space Green's function g and its gradient[4]. The quantity $\vec{t}_+$ in Eq. (18) is the traction vector which is related to $\vec{u}$ by Hooke's law according to

$$\vec{t} = \hat{n} \cdot [\lambda \overset{\leftrightarrow}{I} \nabla \cdot \vec{u} + \mu (\nabla \vec{u} + \vec{u} \nabla)] \tag{19}$$

9

In an invicid fluid the shear modulus, μ, is zero and the Lamé constant λ is simply the compressibility and hence $\vec{t}_+$ becomes the fluid pressure on the surface S.

For the region inside S, the displacement $\vec{u}$, is governed by the following representation

$$\int_S \left\{ \vec{u}_- \cdot [\hat{n} \cdot \overset{\leftrightarrow}{\Sigma}(\vec{r},\vec{r}')] - \overset{\leftrightarrow}{G}(\vec{r},\vec{r}) \cdot \vec{t}_-(\vec{r}') \right\} dS$$

$$= \begin{cases} -\vec{u}_1(\vec{r}) & ; \quad \vec{r} \text{ inside S} \\[2mm] 0 & ; \quad \vec{r} \text{ outside S} \end{cases} \tag{20}$$

where $\overset{\leftrightarrow}{G}$ is the Green's displacement dyadic and $\overset{\leftrightarrow}{\Sigma}$ is the Green's stress dyadic that is related to G by Hooke's law[10].

The incident and scattered displacement fields are expanded in vector spherical functions as follows

$$\vec{u}^o(\vec{r}) = \sum_{n=0}^{\infty} \sum_{m=0}^{n} \sum_{\sigma=1}^{2} a_{nm\sigma} \operatorname{Re} \vec{\psi}_{fnm\sigma}$$

and
$$\tag{21}$$

$$\vec{u}^S(\vec{r}) = \sum_{n=0}^{\infty} \sum_{m=0}^{n} \sum_{\sigma=1}^{2} f_{nm\sigma} \vec{\psi}_{fnm\sigma}$$

where

$$\vec{\psi}_{fnm\sigma} = \nabla \phi_{nm\sigma}(k_f \vec{r}) \tag{22}$$

is the wave function in the fluid.

10

The relevant boundary conditions at S are given by

$$\hat{n}' \cdot \vec{u}'_+ = \hat{n}' \cdot \vec{u}'_- \; ; \; \hat{n}' \cdot \vec{t}'_+ = \hat{n}' \cdot t'_- \; ;$$

$$(\hat{n}' \cdot \vec{t}'_+)_{\text{tangential}} = 0 \quad (\text{r' on S}) \tag{23}$$

Omitting all the details which can be found in Ref. 8, the incident and scattered field coefficients are related through the T-matrix as given by

$$f_{nm} = \sum_{n'm'\sigma'} T_{nm\sigma,n'm'\sigma'} \; a_{n'm'\sigma'} \tag{24}$$

where

$$T = -\text{Re} \; [QR^{-1}P] \; [QR^{-1}P]^{-1} \tag{25}$$

The matrices Q, R and P are given in Ref. 8. The far field scattered amplitude given by Eq. (17) can thus be computed by numerically evaluating the Q, R and P matrices.

III   DISCUSSION OF NUMERICAL RESULTS

The amplitude of the scattered field at distances far from the
scatterer has been calculated for three different geometries a) prolate
spheroid, b) oblate spheroid and c) finite cylinders with spherical end
caps for two types of scatterers namely rigid fixed obstacles and elastic
solid obstacles. The incident wave was taken to be a plane harmonic
wave of frequency ω. Since the obstacles considered have an axis of
revolution which is taken to be the z-axis, without loss of generality
the plane of incidence can be taken to be in the x-z plane and α is
the angle of incidence with respect to the positive z-axis (see Fig. 2).
If $b/a > 1$, the spheroid is prolate and is oblate for $b/a < 1$.

The elements of the Q-matrix in Eq. (14) and the matrices Q, R and P
in Eq. (25) were obtained by Gauss-Legendre quadrature formulas by
using the appropriate equations to describe the surface. The inverse
matrices appearing in the definition of the T-matrix in Eqs. (16) and
(25) were obtained with both the Waterman procedure of orthogonalization
incorporating the symmetry and unitary properties as well as by
straight inversion of the Q-matrix using Gaussian elimination.

In Figs. 3-7, we compare the far field amplitude of the scattered
pressure field for the elastic and rigid prolate spheroid with an
aspect ratio of 2:1. The material properties used in our computations
are given in Table I. Figure 3 is the far field amplitude for $\theta_o = 0°$,
end-on incidence, along the z-axis and $\theta = 90°$, i.e., observation in the
x-y plane. For this scattering geometry it is not possible to distinguish
an elastic spheroid (solid line) from a rigid spheroid (dotted line)

12

in the low $k_f\ell_>$ region ($k_f\ell_> = 0-2$), where $\ell_>$ is half the largest dimension of the scatterer. However, the null at $k_f\ell_> \sim 6.0$ is very sharp for the elastic case and fairly shallow for the rigid case. Figure 4 is the back-scattered pressure field for $\theta_o = 0°$. The maxima and minima come very close and only at the highest value of $k_f\ell_>$ some differences are noticeable. Figure 5 is for $\theta_o = 45°$ and $\theta = 180°$. In Fig. 6, a dramatic difference can be noticed for $\theta_o = 45°$ and $\theta = 135°$ (back scattering). Two prominent peaks are present for the elastic case at $k_f\ell_> \sim 4.0$ and $k_f\ell_> \sim 7.0$ which are absent for the rigid case. In Fig. 7 the back scattered field for $\theta_o = 90°$ is plotted. The elastic scatterer behaves in a noticeably different manner although the difference is not as much as that seen in Fig. 6.

Figures 8-12 compare the scattering from rigid (dotted lines) and elastic (solid line) oblate spheroids of 2:1 aspect ratio. Figure 8 compares the scattered pressure amplitude for $\theta_o = 0°$ and $\theta = 90°$. This figure is very similar to Fig. 3, which is for a prolate spheroid. Again the minima for the elastic case are more noticeable than for the rigid case. Figure 9 is the comparison of the back scattered field for $\theta_o = 0°$. It is seen that the behavior of the elastic oblate spheroid is significantly different from that of a rigid one. Figure 10 is the bistatic amplitude for $\theta_o = 45°$ and $\theta = 180°$. The elastic spheroid has a very pronounced minimum at $k_f\ell_> \sim 5.3$ which is absent for the rigid case. The back scattered field for $\theta_o = 45°$ shown in Fig. 11 is also dramatically different for rigid and elastic boundary conditions. Finally, for the oblate spheroid back scattering at $\theta_o = 90°$ is compared for the rigid and elastic cases in Fig. 12. Although there are differences, it is not as much as for $\theta_o = 45°$.

13

Figures 13-17 are for the finite circular cylinder of length 2h capped by hemispheres of radius 'a' at either end, see Fig. 2. The plots are of the scattered pressure versus $k_f\ell$ where ℓ = h+a, the half length of the cylinder. The bistatic ($\theta = 90°$ in the x-y plane) and backscattered fields for $\theta_o = 0°$ are almost identical for the rigid and elastic cases, see Figs. 13 and 14, except at $k_f\ell \sim 6.0$ where elastic obstacle shows a sharp null in the bistatic amplitude. For $\theta_o = 45°$, the bistatic field for $\theta = 180°$ (Fig. 15) displays a sharp minimum at $k_f\ell \sim 6.0$ for the elastic obstacle whereas a maximum can be noticed at the same wavenumber for the rigid obstacle. The back scattered field for $\theta_o = 45°$ displays a very prominent maximum at $k_f\ell \sim 4.0$ and a minimum at $k_f\ell \sim 5.5$ for the elastic finite cylinder which are absent in the rigid case, see Fig. 16. It is interesting to observe from Figs. 6 and 16 that the position of the peak ($k_f\ell \sim 4.0$) is the same for the prolate spheroid and the finite cylinder. However. the peak present at $k_f\ell_> \sim 7.0$ for the prolate spheroid is absent in Fig. 16. The backscattered field for the rigid finite cylinder at $\theta_o = 90°$ differs noticeably from the elastic case as depicted in Fig. 17. In Figs. 7 and 17, we note a striking similarity in the back scattered far field for $\theta_o = 90°$ between prolate spheroid and finite cylinder of the same aspect ratio.

In general it is noticed from the data that the position of the first peak is the same for rigid and elastic scatterers and that the peak is higher for the rigid body for all geometries. It has also been noticed that as the properties of the elastic obstacles approach that of a rigid body as in the case of tungsten - carbide[6], the scattered fields have the same value as that of rigid body. From the studies made thus far,

14

it would appear that one can infer a wealth of information on the geometry

of an elastic body by calculations on a rigid body of the same shape for

the frequency range considered. The calculations for the rigid case are

of course many times less expensive and more accurate. However, we have

observed (Figs. 6, 9, 10 and 16) that the above statement is not true at

certain frequencies dependent on the scattering geometry and shape at

which the elastic case differs widely from the corresponding rigid case.

These prominent differences as seen in Figs. 6, 9, 10 and 16 are closely

related to the resonance phenomena of submerged elastic objects and need

further study and explanation. The numerical results for the elastic

case are correct and have been verified by experiments, see Refs. 9 and 17.

The scattering from a rigid body for all angles of incidence may be

easily explained on the basis of creeping wave analysis[3]. The frequency

dependence is a periodic damped oscillation. Although a creeping wave

pattern is noticeable even for the elastic scatterer, the pattern is not

as regular and breaks down for certain scattering geometries.

ACKNOWLEDGMENTS

REFERENCES

1. R. Hickling, J. Acoust. Soc. Am. 34, 1582 (1962)

2. W.G. Neubauer, J. Acoust. Soc. Am. 45, 1134 (1969)

3. Louis R. Dragonette, Evaluation of the relative importance of circumferential or creeping waves in the acoustic scattering from rigid and elastic solid cylinders and from cylindrical shells (Naval Research Laboratory Report 8216, 1978)

4. O.D. Grace and R.R. Goodman, J. Acoust. Soc. Am. 39, 173 (1966)

5. R.E. Bunney, R.R. Goodman and S.W. Marshall, J. Acoust. Soc. Am. 46, 1223 (1969)

6. Richard H. Vogt and Werner G. Neubauer, J. Acoust. Soc. Am. 60(1), 15 (1976).

7. A. Boström, J. Acoust. Soc. Am. 67, 390 (1980)

8. B. Peterson, V.V. Varadan and V.K. Varadan, Int. J. Wave Motion 2, 23 (1980)

9. J.H. Su, V.V. Varadan, V.K. Varadan and L. Flax, J. Acoust. Soc. Am. 68, 686 (1980)

10. V.K. Varadan and V.V. Varadan (Eds.) Acoustic, Electromagnetic and Elastic Wave Scattering - Focus on the T-matrix Approach (Pergamon Press, New York 1980)

11. J.J. Bowman, T.B.A. Senior and P.L.E. Uslenghi (Eds.) Electromagnetic and Acoustic Scattering by Simple Shapes (North-Holland Publishing Company, Amsterdam 1969)

12. R.D. Spence and Sara Granger, J. Acoust. Soc. Am. 23(6), 701 (1951)

13. Louis R. Dragonette, Richard H. Vogt, Lawrence Flax and W.G. Neubauer, J. Acoust. Soc. Am. 55, 1130 (1974)

14. M.S. Lang, An Experimental Analysis of the Basic Phenomena Involved in Modern Diffraction Theories (Ph.D. Thesis, Pensylvania State University, 1980)

15. A. Freedman, J. Sound and Vibration 52, 265 (1977)

16. P.C. Waterman, J. Acoust. Soc. Am. 45, 1417 (1969)

17. S.K. Numrich and V.V. Varadan, J. Acoust. Soc. Am.

TABLE I. Material properties used in computations.

	Water	Aluminum
Density (g/cm^3)	1.00	2.70
Compressional wave speed (X 10^{-5} cm/s)	1.482	6.376
Shear wave speed (X 10^{-5} cm/s)	0	3.12
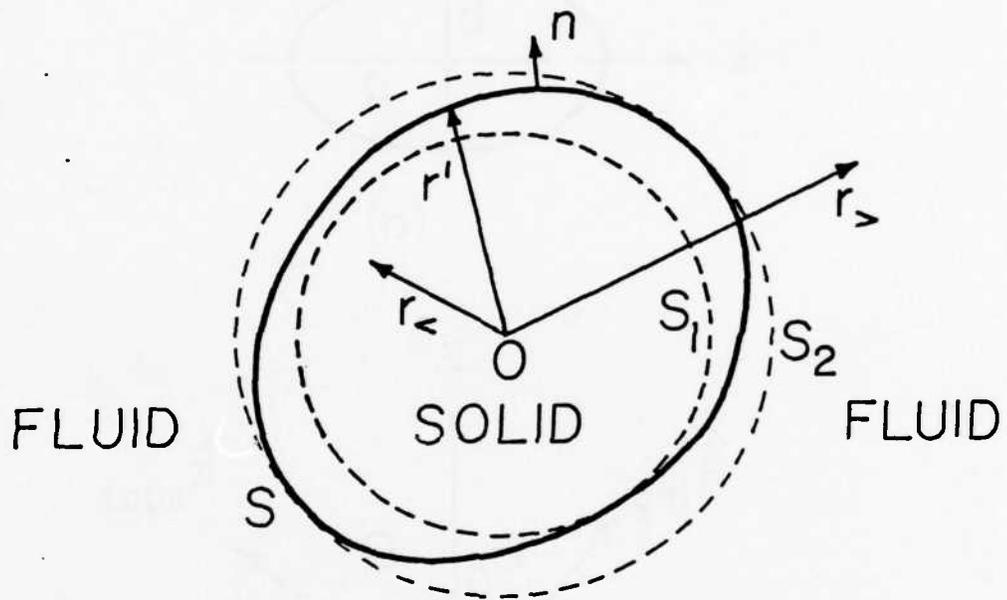
Figure 1: Solid in a fluid

19
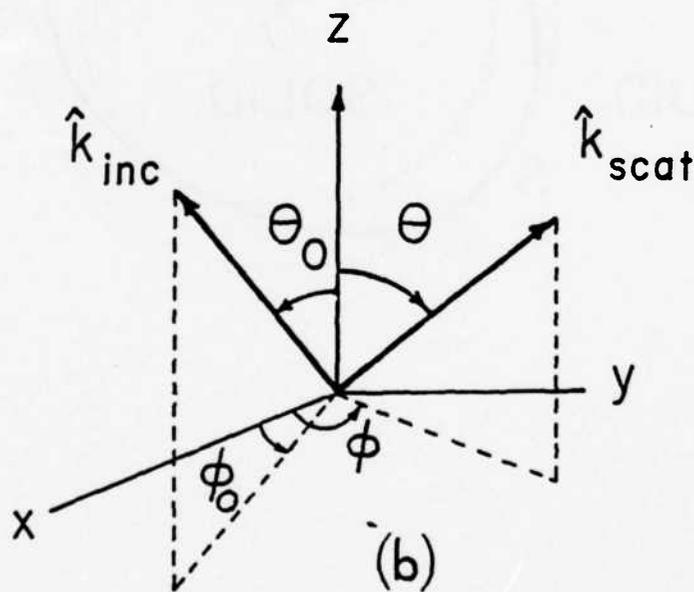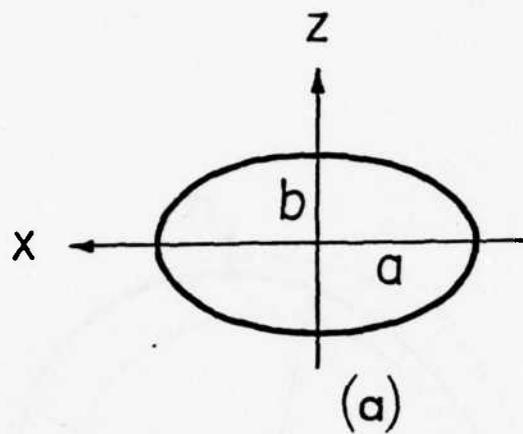
Figure 2a: Homogeneous solid spheroid

Figure 2b: Scattering geometry

20
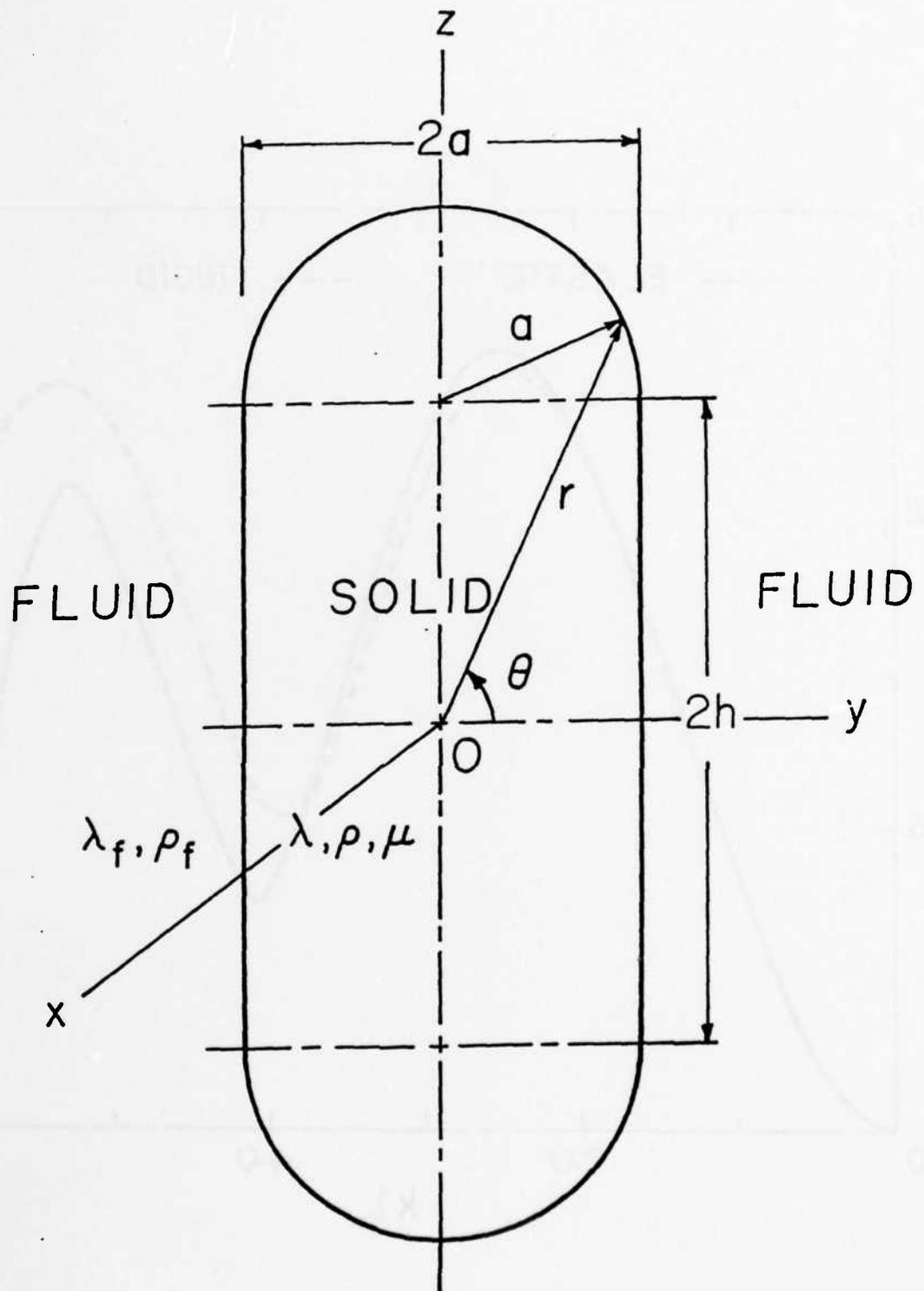
Figure 2c: Homogeneous finite cylinder
with hemispherical end caps

21
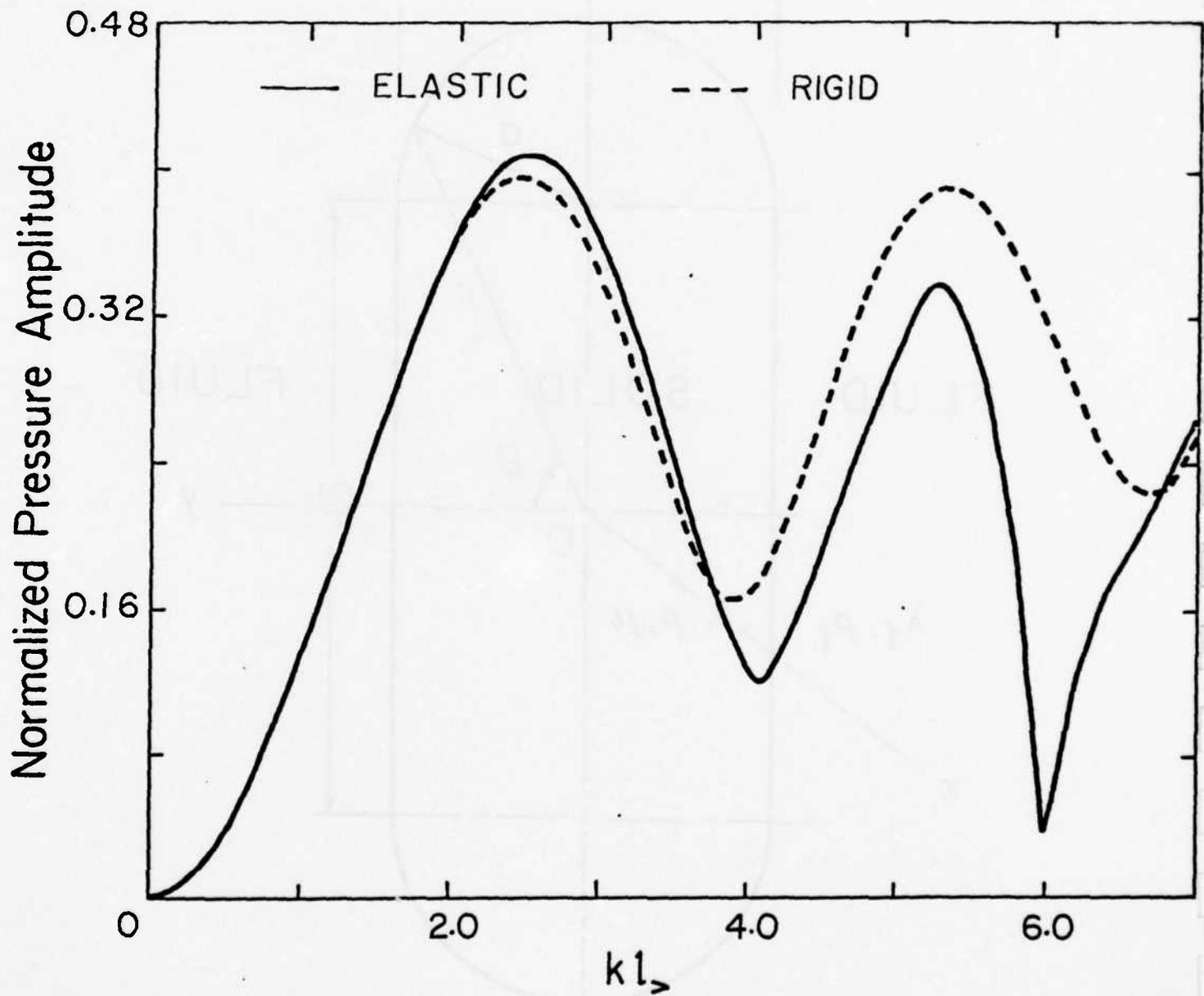
Figure 3 : Bistatic scattering amplitude ($\theta=90°$) vs. $k_f \ell_>$ for a prolate spheroid for $\theta_o=0°$
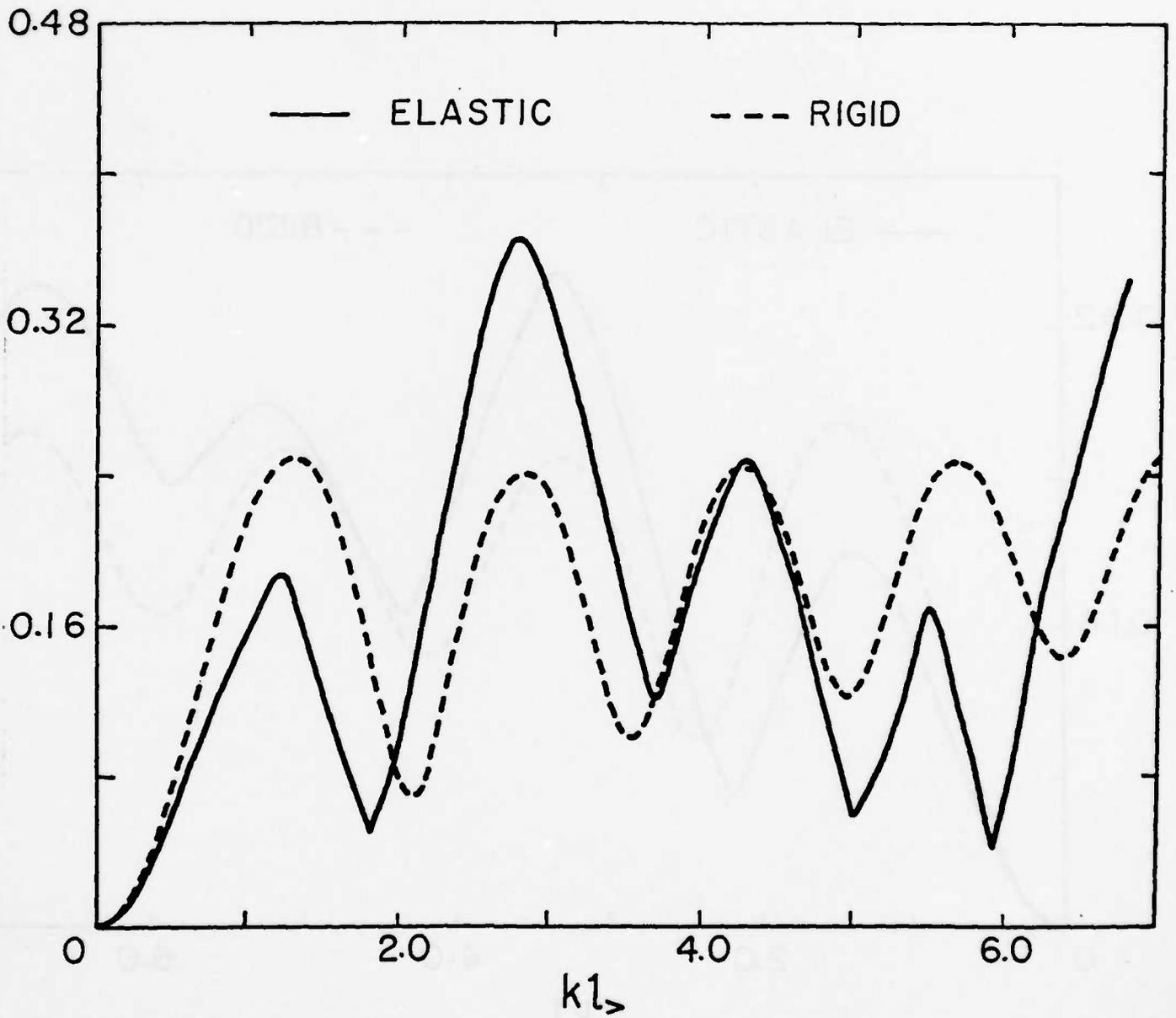
Figure 4: Back scattering amplitude vs. $k_f l_>$ for a prolate spheroid for $\theta_o = 0°$
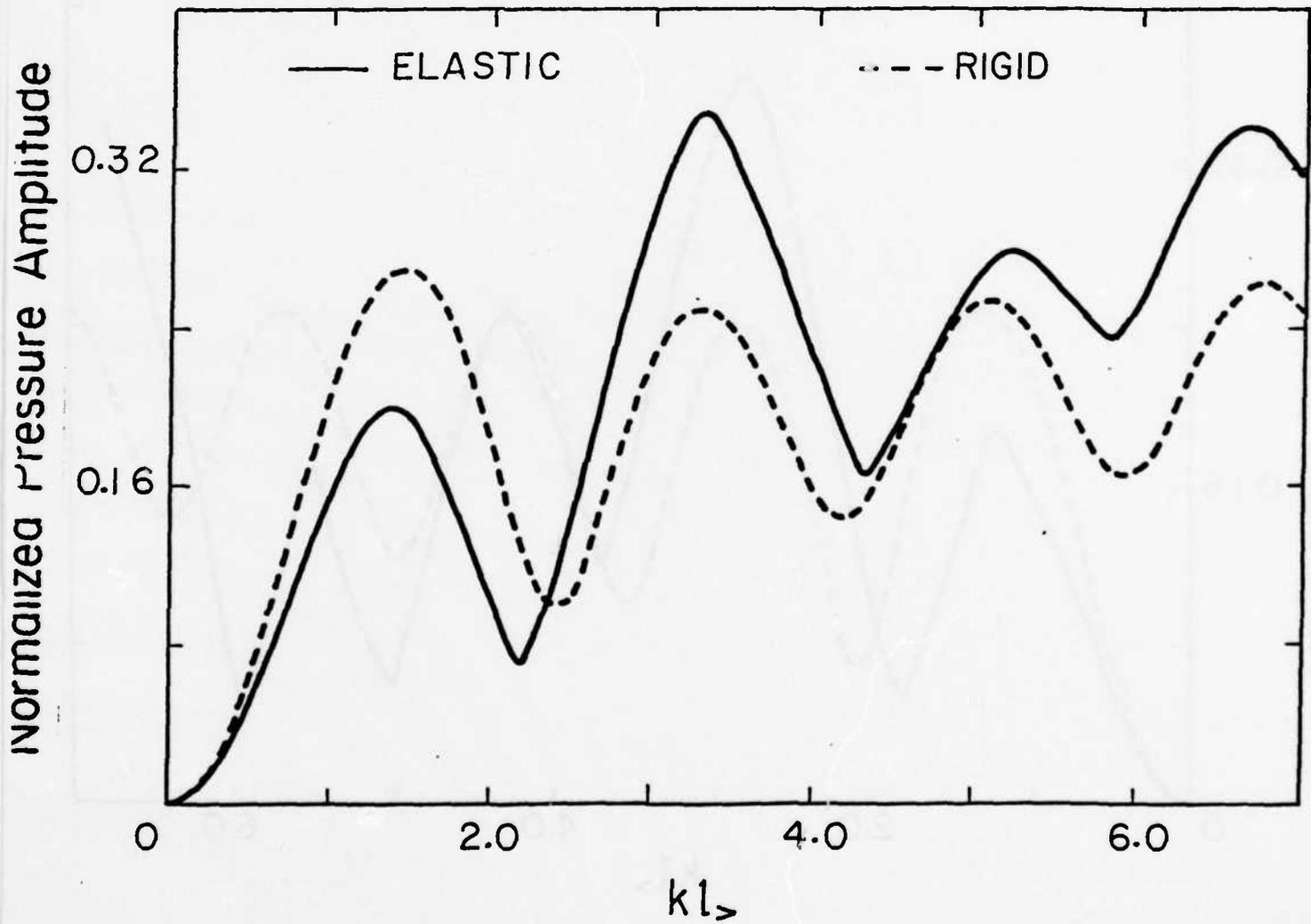
Figure 5: Bistatic scattering amplitude ($\theta = 180°$) vs. $k_f \ell_>$ for a prolate spheroid for $\theta_o = 45°$
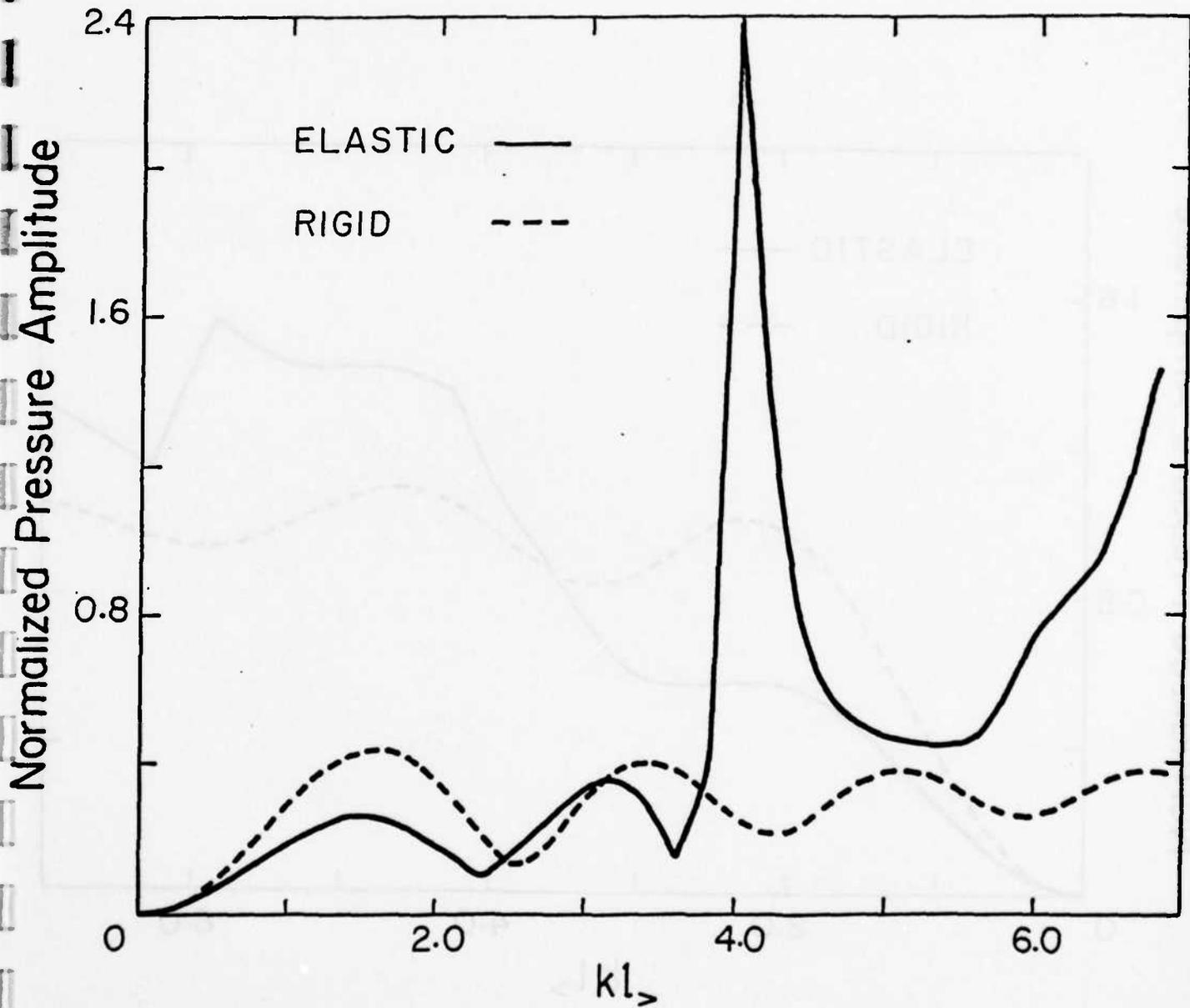
Figure 6: Back scattering amplitude vs. $k_f \ell_>$ for a prolate spheroid for $\theta_o = 45°$

25
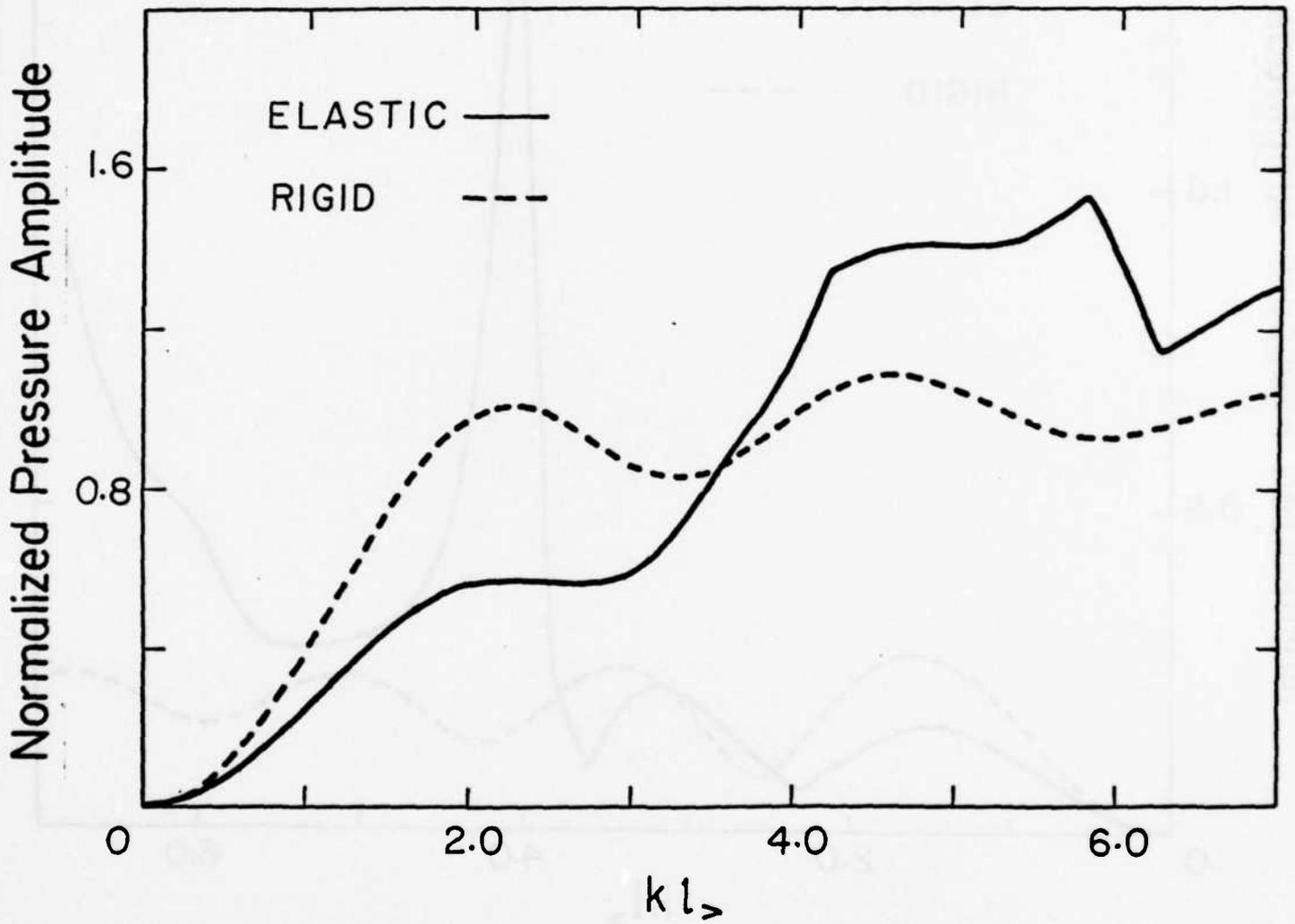
Figure 7: Back scattering amplitude vs. $k_f \ell_>$ for a prolate spheroid for $\theta_o = 90°$
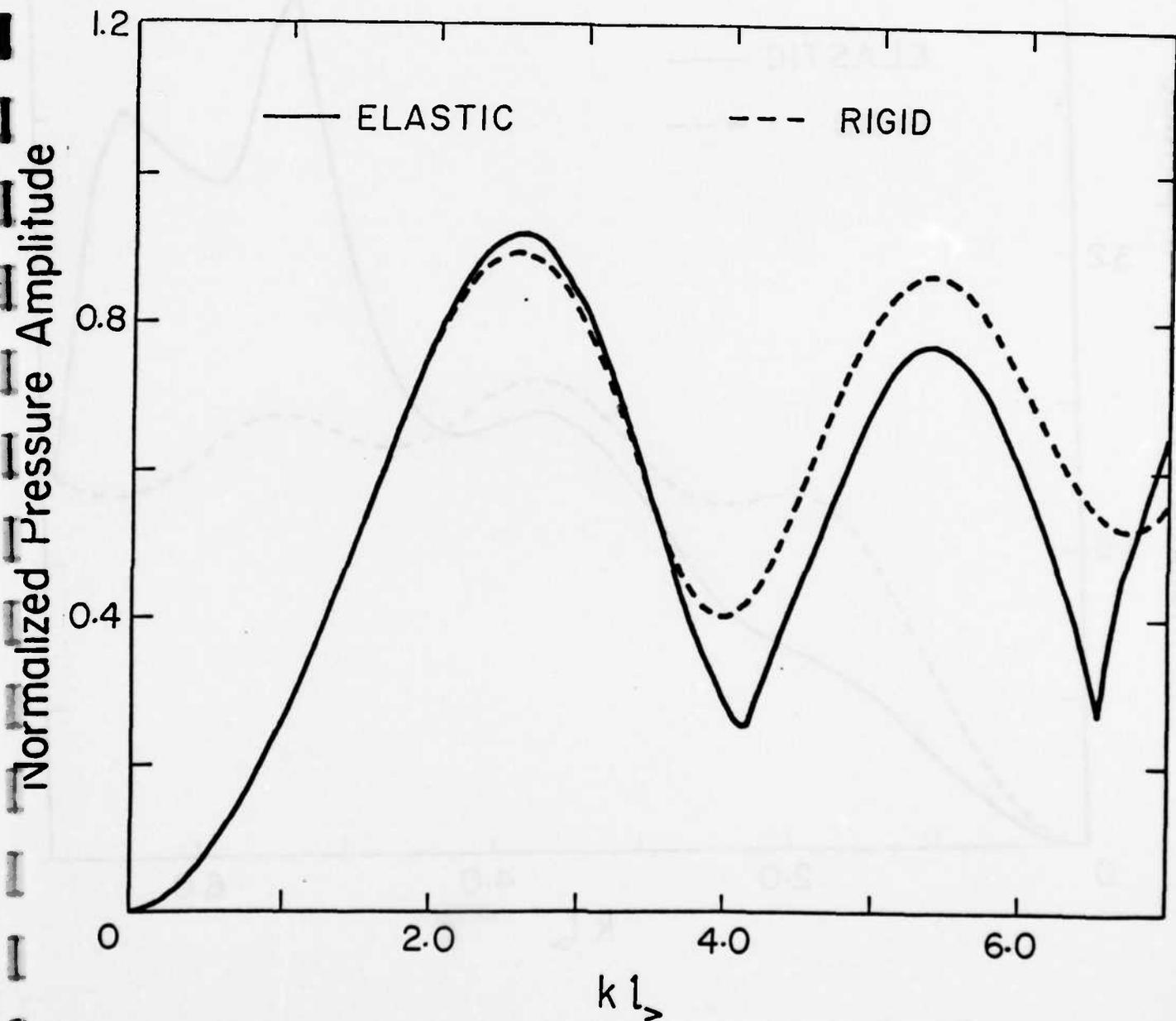
Figure 8: Bistatic scattering amplitude ($\theta=90°$) vs. $k_f l_>$ for an oblate spheroid for $\theta_o=0°$

27
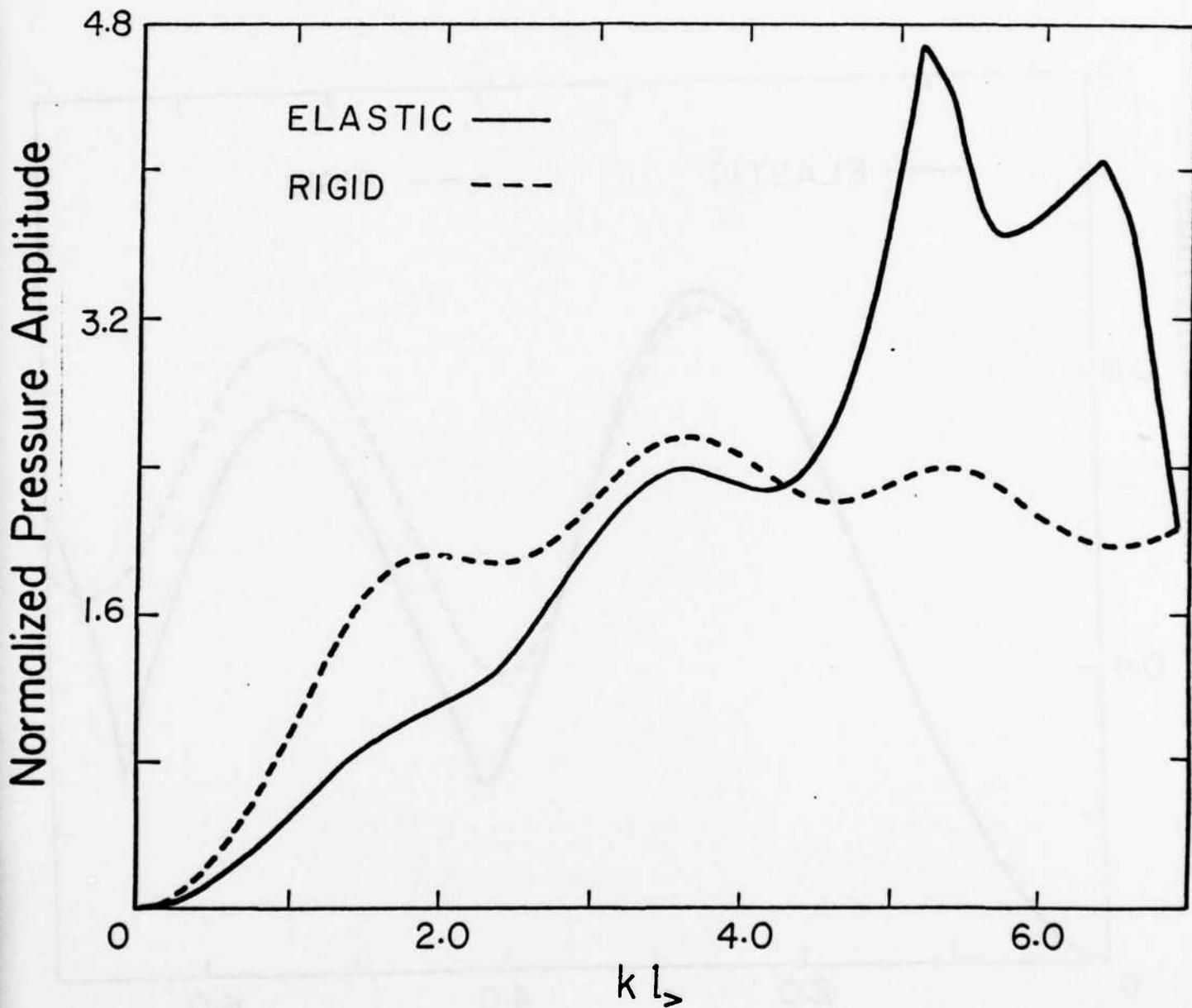
Figure 9: Back scattering amplitude vs. $k_f \ell_>$ for an oblate spheroid for $\theta_o = 0°$

28
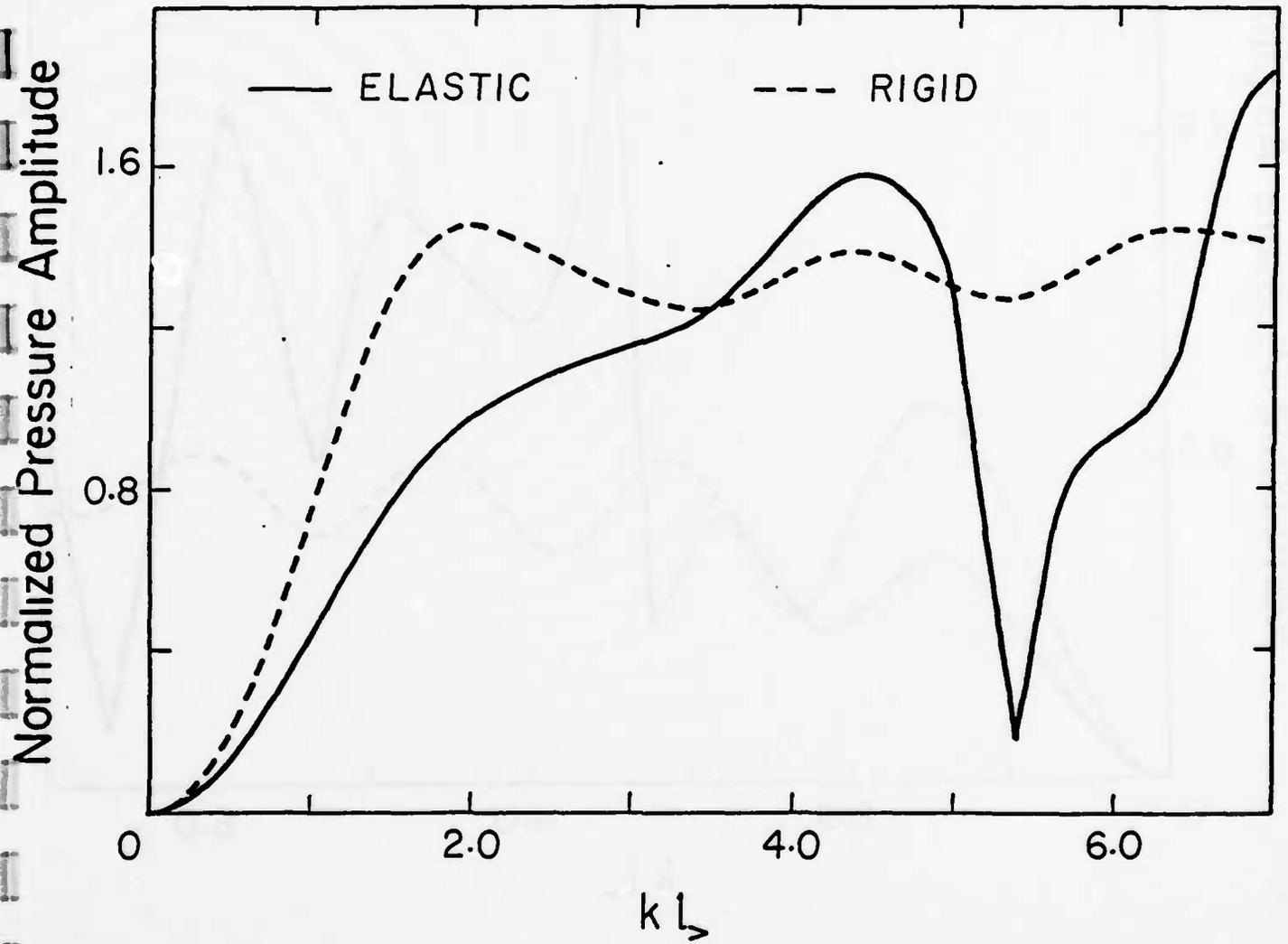
Figure 10: Bistatic scattering amplitude ($\theta = 180°$) vs. $k_f \ell_>$ for an oblate spheroid for $\theta_o = 45°$
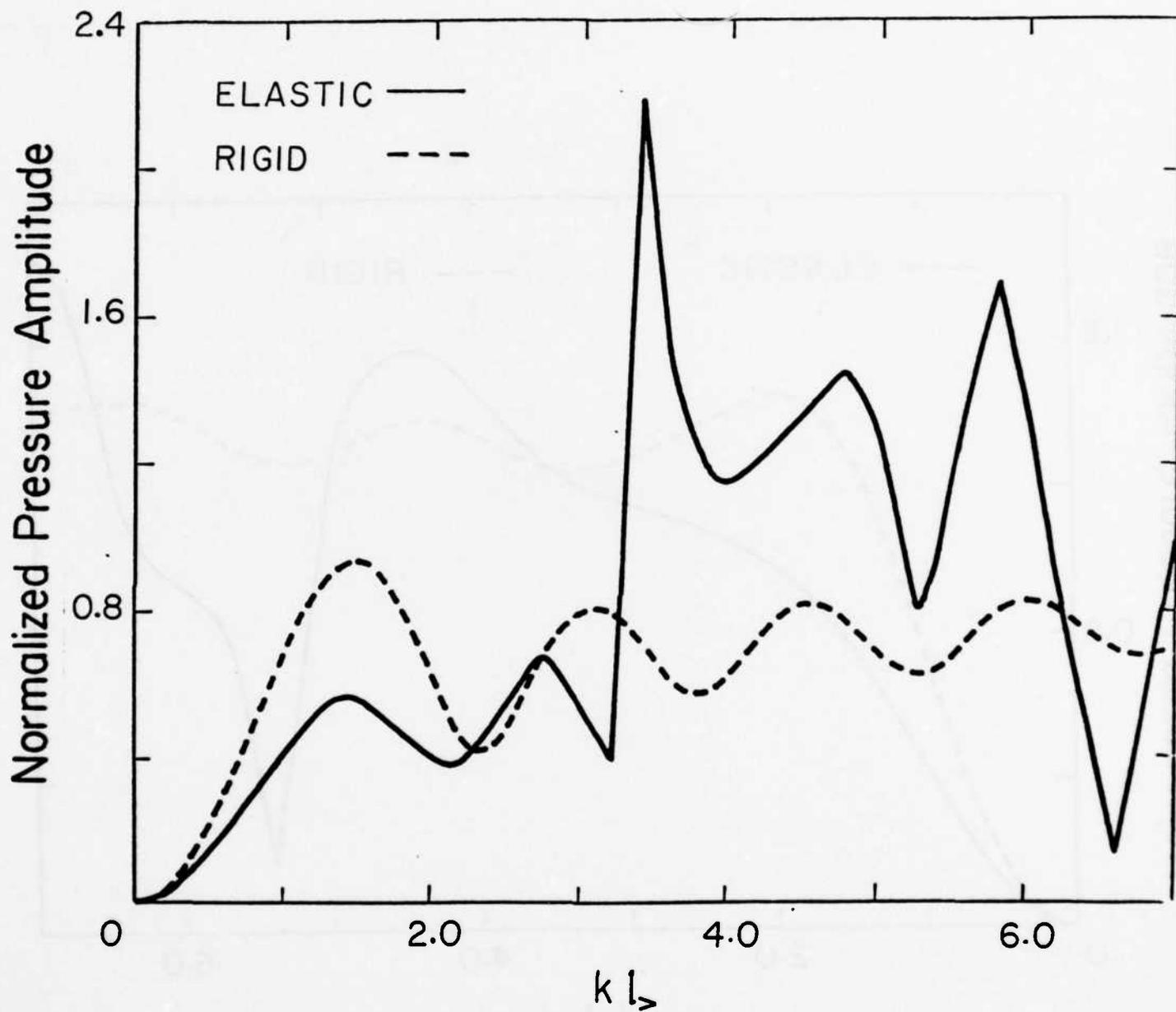
Figure 11: Back scattering amplitude vs. $k_f \ell_>$ for an oblate
spheroid for $\theta_o = 45°$

30
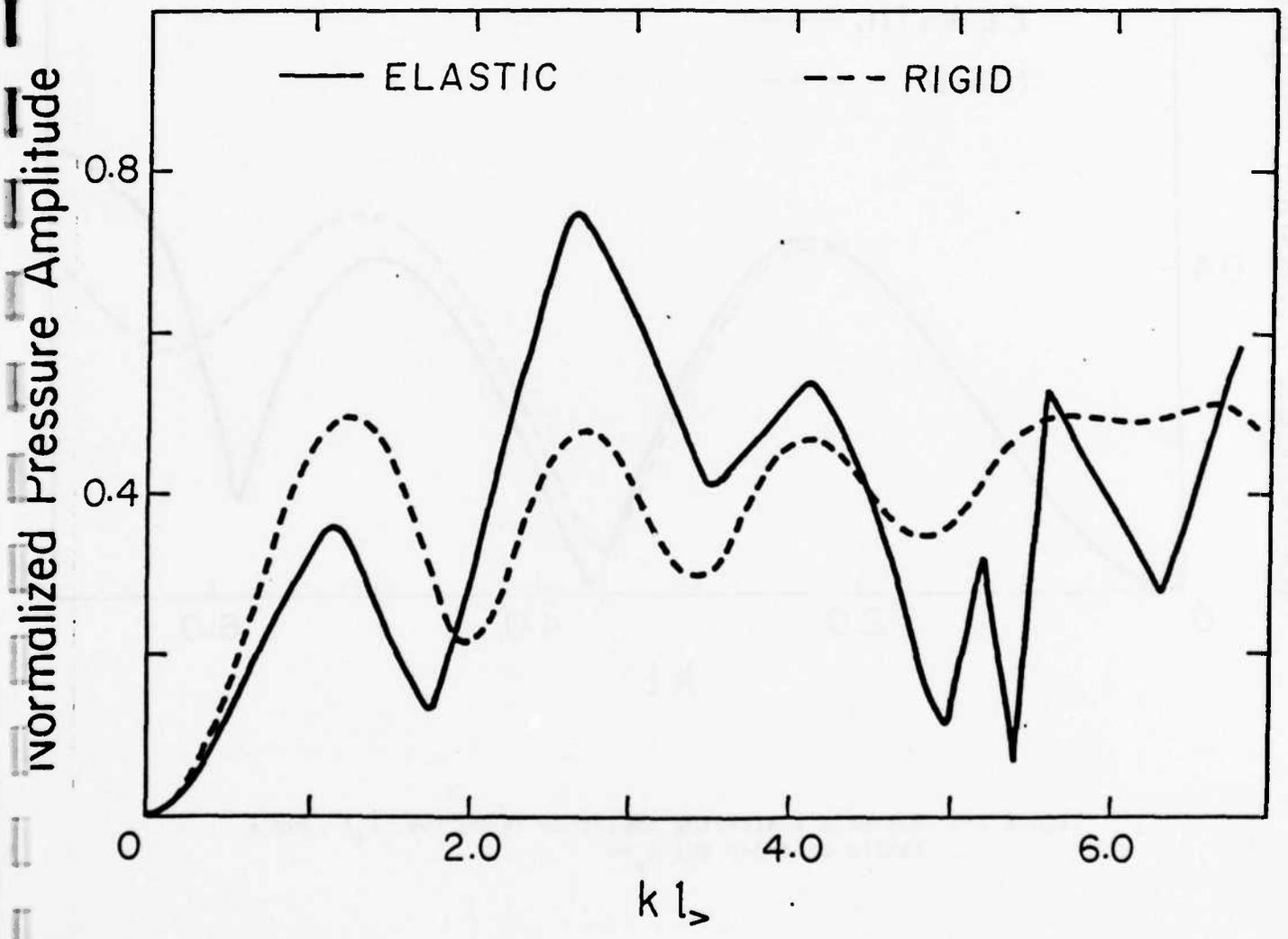
Figure 12: Back scattering amplitude vs. $k_f \ell_>$ an oblate spheroid for $\theta_o = 90°$

31
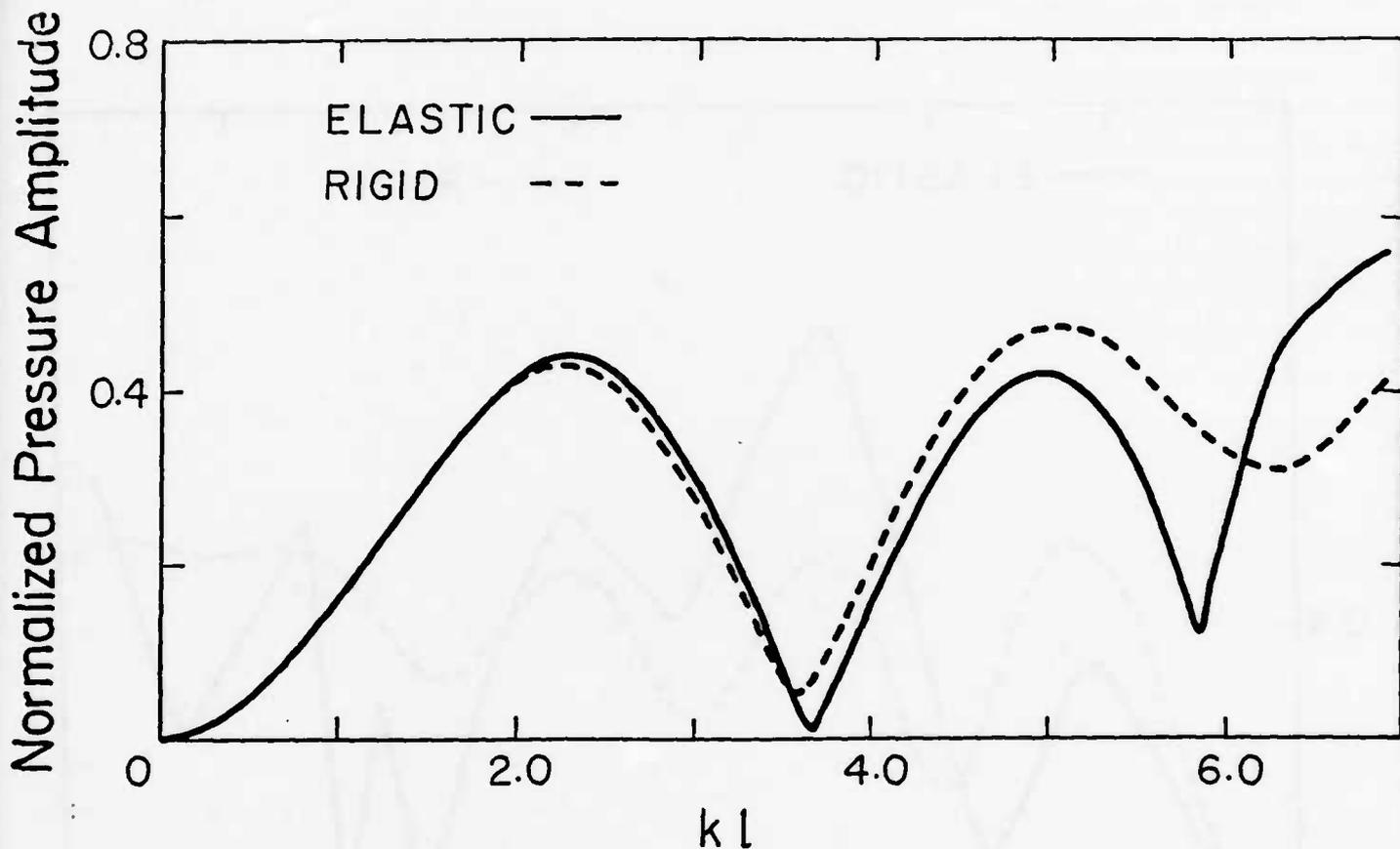
Figure 13: Bistatic scattering amplitude ($\theta = 90°$) vs. $k_f \ell$ for a finite cylinder for $\theta_0 = 0°$
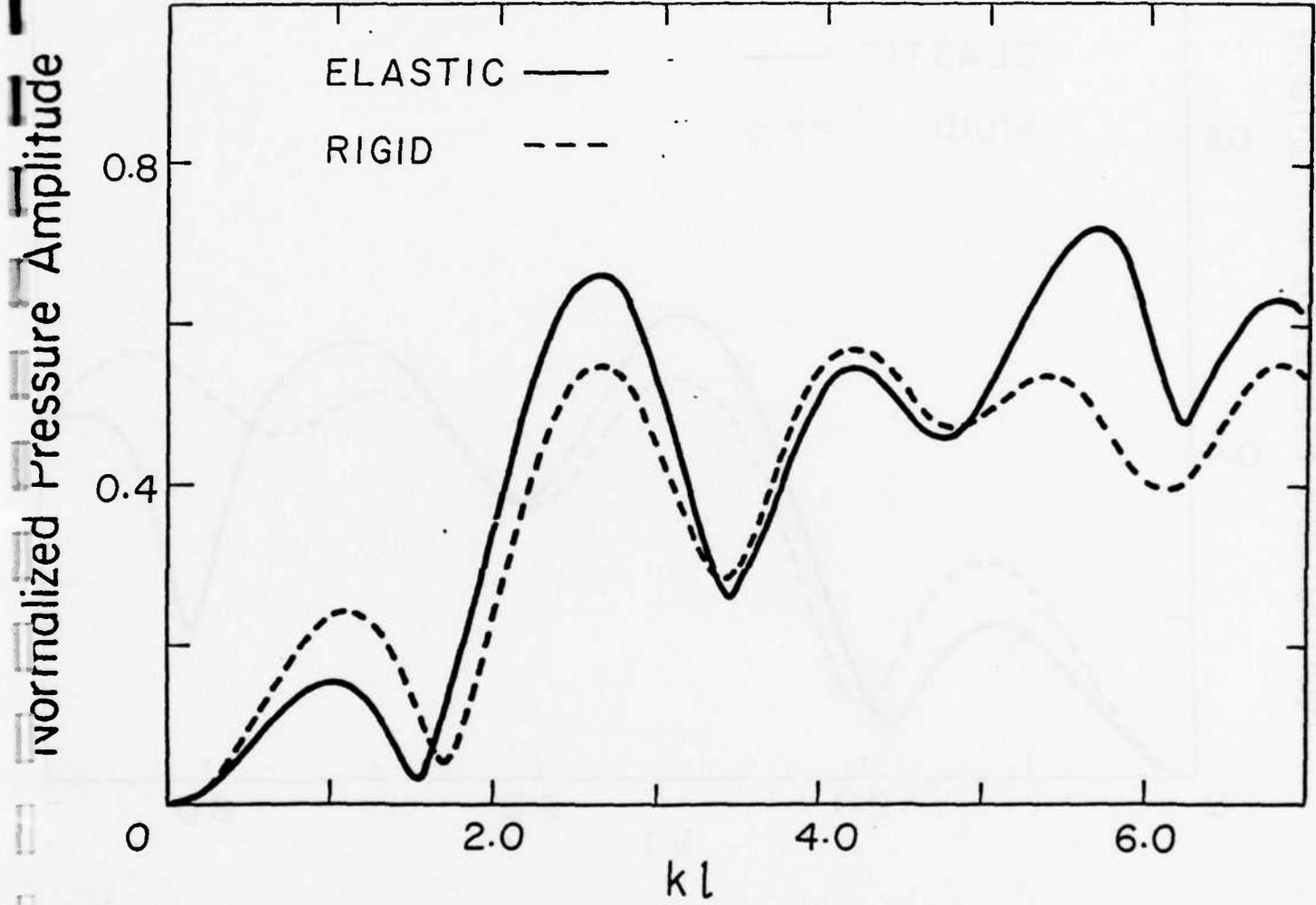
Figure 14: Back scattering amplitude vs. $k_f \ell$ for a finite cylinder for $\theta_o = 0°$
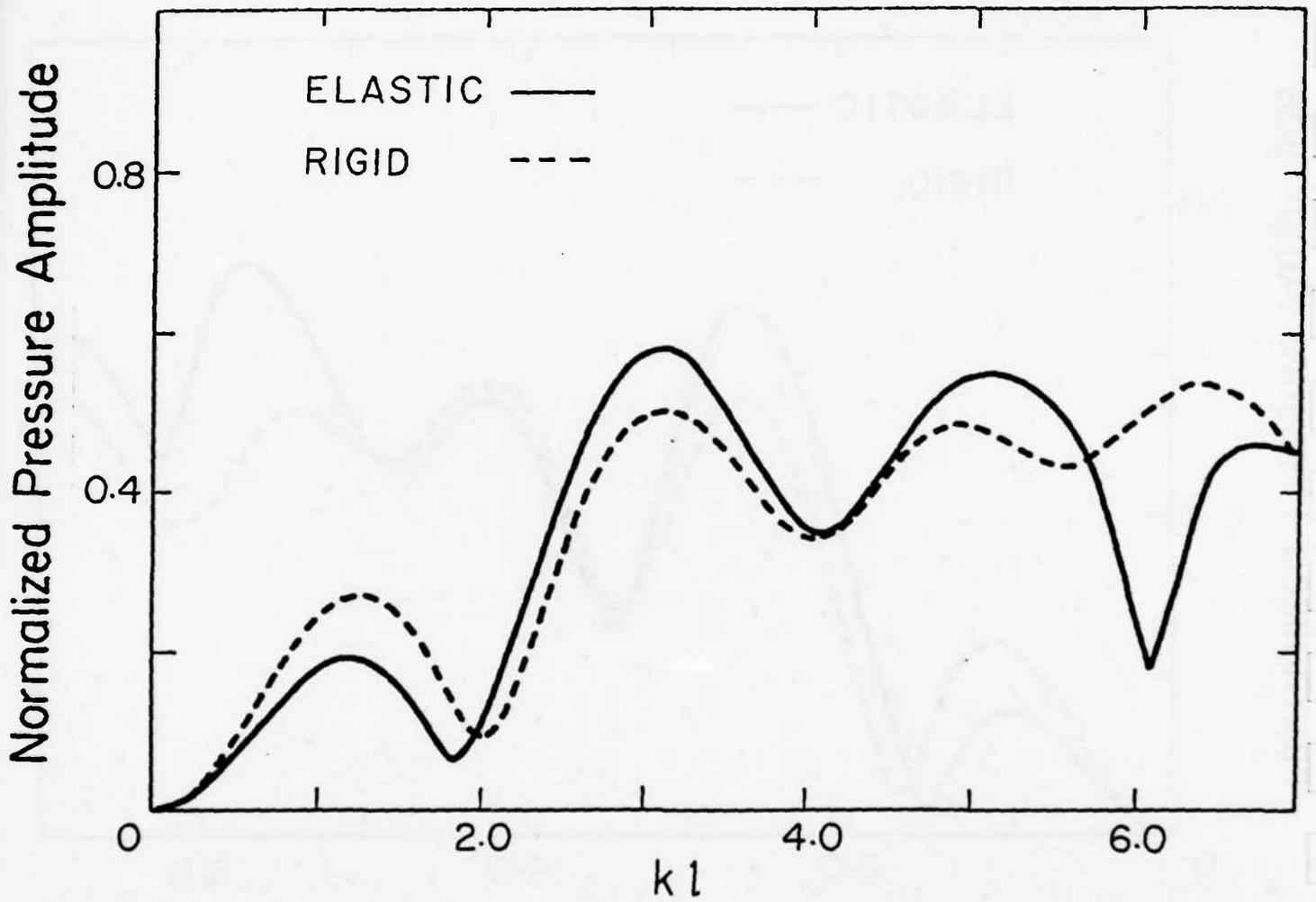
Figure 15: Bistatic scattering amplitude ($\theta = 180°$) vs. $k_f \ell$ for a finite cylinder for $\theta_o = 45°$
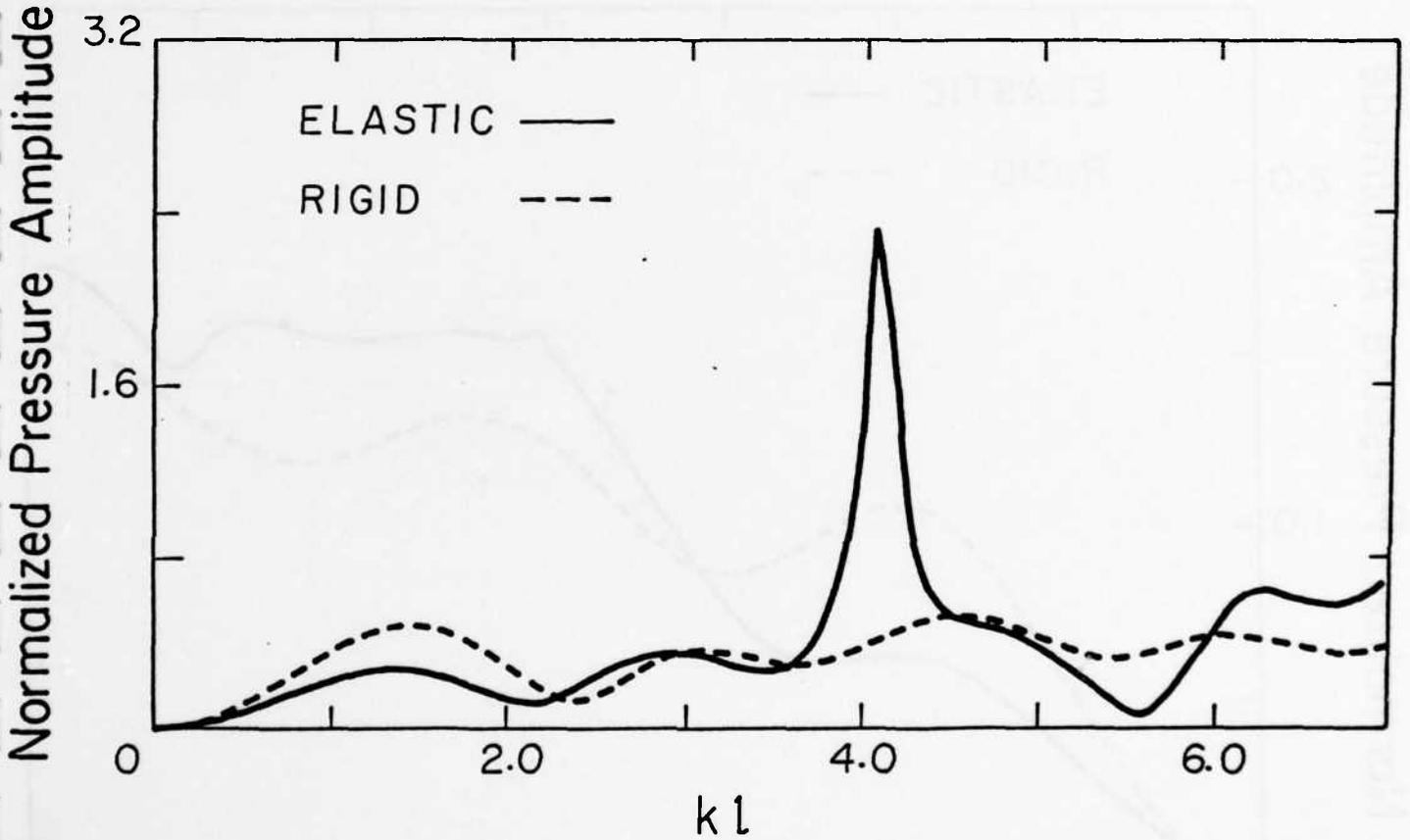
Figure 16: Back scattering amplitude vs. $k_f\ell$ for a finite cylinder for $\theta_o = 45°$
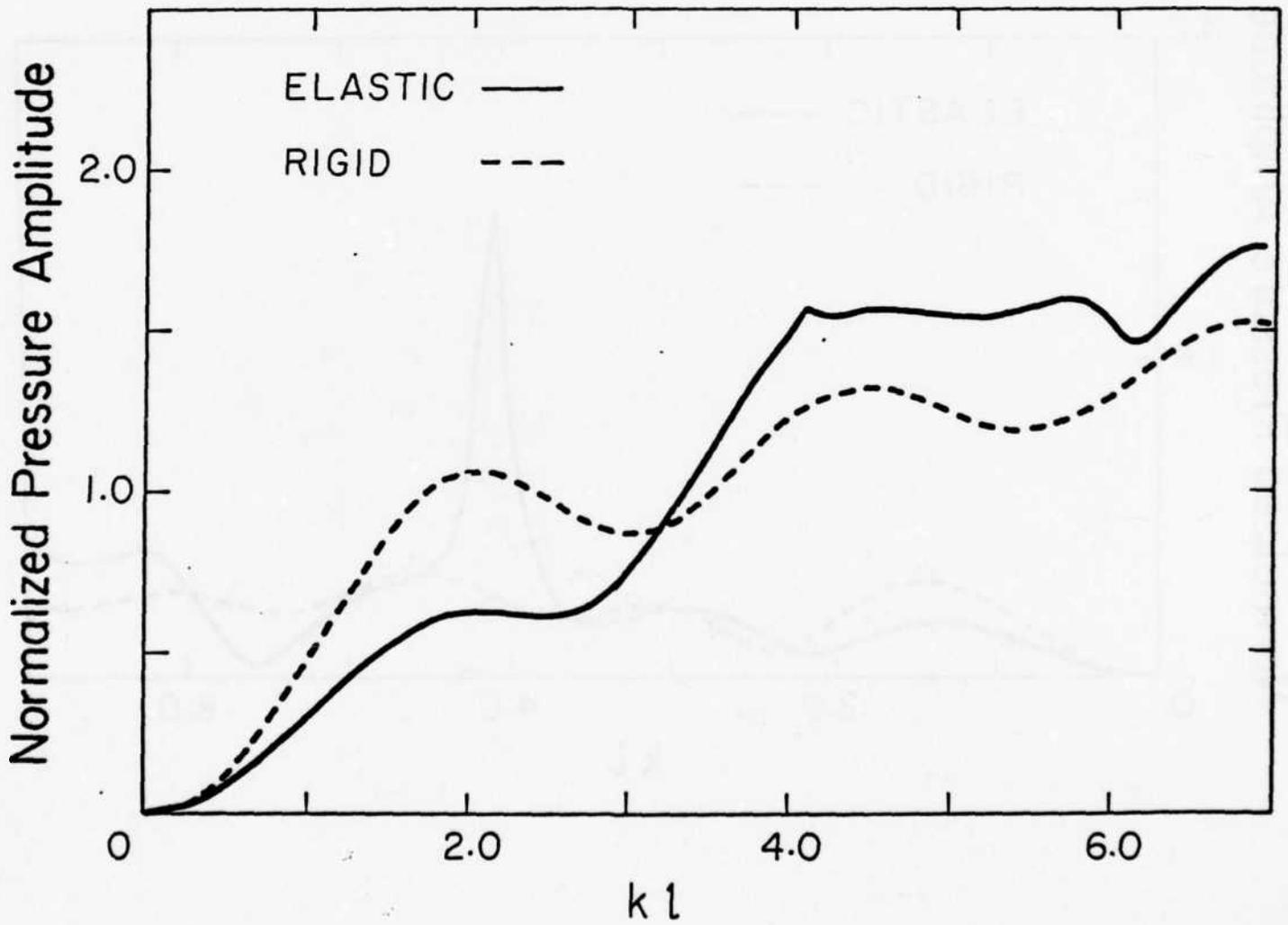
Figure 17: Back Scattering amplitude vs. $k_f\ell$ for a finite cylinder for $\theta_0 = 90°$

Coherent Wave Attenuation by a Random Distribution of Particles [†]

by

V.N. Bringi[1], V.V. Varadan[2] and V.K. Varadan[2]
Wave Propagation Group, Boyd Laboratory
The Ohio State University
Columbus, Ohio 43210

ABSTRACT

The coherent electromagnetic wave attenuation in an infinite medium
composed of a random distribution of identical, finite scatterers is
studied. A self-consistent multiple scattering theory using the T-matrix
of a single scatterer and a suitable averaging technique is employed. The
statistical nature of the position of scatterers is accounted for by ensemble
averaging. This results in a hierarchy of equations relating the different
orders of correlations between the scatterers. Lax's quasicrystalline
approximation (QCA) is used to truncate the hierarchy enabling passage to
a homogeneous continuum whose bulk propagation characteristics such as
phase velocity and coherent wave attenuation can then be studied. Three
models for the pair correlation function are considered. The Matern
model and the well stirred approximation (WSA) are good only for sparse
concentrations, while the Percus-Yevick approximation (P-YA) is good for
a wider range of concentration. The results obtained using these models
are compared with the available experimental results for dielectric
scatterers embedded in another dielectric medium. Practical applications
of this study include radar meterology and communications through
hydrometers, dust, vegetation, etc.

1. INTRODUCTION

We consider the propagation of plane coherent electromagnetic waves
in an infinite medium containing identical, lossless randomly distributed
particles. Our aim is to characterize the random medium by an effective
complex wave number K which would be a function of the particle concentration,
electrical size and the statistical description of the random positions of
the scatterers. The imaginary part of K describes the coherent attenuation
which is due to multiple scattering only since the particles themselves
are assumed to be lossless. The understanding of the behavior of Im(K) as
a function of particle concentration c and/or frequency ka is very
important in many practical applications, including wave propagation in
the atmosphere and oceans and whenever distribution of random scatterers
influence electromagnetic wave behavior.

The theoretical formulation presented here closely follows the
procedure described in Varadan et. al. [1979] and Bringi et. al. [1981].
This approach is based on a self-consistent multiple scattering theory
and relies on the T-matrix [Waterman 1971] which relates the field
scattered by a particle to an arbitrary exciting field. The statistical
description of the random position of the scatterers is used to define a
configurational average which results in a hierarchy of equations relating
the different orders of correlations between the scatterers. Lax's
[1952] quasi-crystalline approximation is used to truncate the hierarchy
which results in the usual "hole-correction" integrals. Following Twersky
[1977, 1978 a,b], a radially symmetric pair-correlation function is
introduced and approximate models are chosen from Talbot and Willis [1980].

The "well-stirred" approximation (WSA) was used previously by Varadan et. al. [1979] and Bringi et. al. [1981] which assumes no correlation between the particles except that they should not inter-penetrate. In particular, the WSA gives unphysical results for $c \geq 0.125$ at the Raleigh or low frequency limit.

In this paper, we consider two other pair-correlation functions, viz. (i) the Matern [1960] model and (ii) the Percus-Yevick [1957] model for a classical system of hard spheres. Computations of $Im(K)$ are presented for dielectric scatterers in a dielectric medium, using the above three models as a function of frequency and concentration. We also compare our solution to some recent optical propagation experiments conducted by Ishimaru [1981]. Sample computations are also presented comparing the WSA and the single scattering approximation for a rain medium.

2. FORMULATION OF THE PROBLEM

Consider N identical, finite dielectric scatterers that are randomly distributed either in free space or in a different dielectric medium. The scatterers are homogeneous with a relative dielectric constant of ϵ_r, their centers being denoted by 0_1, 0_2, 0_3, ..., 0_N. They are assumed to be bodies of revolution with symmetry axis parallel to the z-direction. Monochromatic plane coherent electromagntic wave is assumed to propagate along the symmetry axis of the scatters to satisfy the condition that the effective medium be isotropic and polarization insensitive. The time dependence of the incident field and hence the fields scattered by the individual scatterers is all of the form $\exp(-j\omega t)$ and this is suppressed in the equations that follow.

Even though the theory presented here is valid for spheroidal scatterers [Varadan, et. al. 1981], we present numerical results only for spherical scatterers in order to compare our results with available experiments.

Let $\vec{E}^0(\vec{r})$ be the electric field arising from the incident plane wave and $\vec{E}_i^S(\vec{r})$ the field scattered by the i-th scatterer. Both these fields satisfy the vector Helmholtz equation. The problem at hand reduces to computing the total wave field at any point outside the scatterers, satisfying the appropriate boundary condition on the surface of the scatterers and radiation conditions at infinity.

The total field at any point outside the scatterers can be interpreted as the sum of the incident field and the fields scattered by all the scatterers, which can be written as

$$\vec{E}(\vec{r}) = \vec{E}^0(\vec{r}) + \sum_{i=1}^{N} \vec{E}_i^S(\vec{\rho}_i) \quad ; \quad \vec{\rho}_i = \vec{r} - \vec{r}_i \tag{1}$$

where $\vec{E}_i^S(\vec{\rho}_i)$ is the field scattered by the i-th scatterer at the observation point $\vec{r}$. However, the field that excites the i-th scatterer is the incident field $\vec{E}^0$ plus the fields scattered from all other scatterers except the i-th. The term exciting field $\vec{E}^e$ is used to distinguish between the field actually incident on a scatterer and the external incident field $\vec{E}^0$ produced by a source at infinity. Thus, at a point $\vec{r}$ in the vicinity of the i-th scatterer, we write

$$\vec{E}_i^e(\vec{r}) = \vec{E}^0(\vec{r}) + \sum_{j \neq i}^{N} \vec{E}_j^S(\rho_j) \quad ; \quad a \leq |\rho_j| < 2a \tag{2}$$

where 'a' is a typical dimension of the scatterer.

The exciting and scattered fields for each scatterer can be expanded in terms of vector spherical functions with respect to an origin at the center of that scatterer:

$$\vec{E}_i^e(\vec{r}) = \sum_{\tau=1}^{2} \sum_{\ell=1}^{\infty} \sum_{n=0}^{\ell} \sum_{\sigma=1}^{2} b_{\tau\ell n\sigma}^i \, \text{Re} \, \vec{\psi}_{\tau\ell n\sigma}(\vec{\rho}_i)$$

$$\tag{3}$$

$$= \sum_{\tau n} b_{\tau n}^i \, \text{Re} \, \vec{\psi}_{\tau n}^i$$

$$\vec{E}_i^S(\vec{r}) = \sum_{\tau n} B_{\tau n}^i \, \vec{\psi}_{\tau n}^i \tag{4}$$

where the vector spherical functions are defined as

$$\vec{\psi}_{1\ell n\sigma}(\vec{r}) = \nabla \times [\vec{r} \, h_\ell^{(1)}(kr)] \, Y_{\ell n\sigma}(\theta,\phi) \tag{5}$$

$$\vec{\psi}_{2\ell n\sigma}(\vec{r}) = \frac{1}{k} \nabla \times \vec{\psi}_{1\ell n\sigma}(\vec{r}) \; . \tag{6}$$

In equations (3-6), k is the wave number; $h_\ell^{(1)}$ is the Hankel function of the first kind and the $Y_{\ell n\sigma}(\theta,\phi)$ are the normalized spherical harmonics defined with real angular functions. In Equation(3), the exciting field is expanded in terms of the regular (Re) basis set (Re $\vec{\psi}_{\tau n}^i$) obtained by replacing $h_n^{(1)}$ in Equations (5-6) by j_n, the spherical Bessel functions of the first kind. Thus, the choice of the basis set in Equation (4) satisfies the radiation condition at infinity for the scattered field, while the choice in (3) satisfies the

regular behavior of the exciting field in the region $a < |\vec{\rho}_i| < 2a$. The superscript i on the basis functions refer to expansions with respect to 0_i, and $b_{\tau n}^i$ and $B_{\tau n}^i$ are the unknown exciting and scattered field coefficients. We also expand the incident field in terms of vector spherical functions:

$$\vec{E}^0(\vec{r}) = e^{ik\hat{z}\cdot\vec{r}_i} \sum_{\tau n} a_{\tau n} \text{ Re } \vec{\psi}_{\tau n}^i(\vec{\rho}_i) \tag{7}$$

where $a_{\tau n}$ are the known incident field coefficients.

The unknown coefficients $b_{\tau n}^i$ can be related to $B_{\tau n}^i$ by means of any convenient scattering operator, in this case we employ the T-matrix as defined by Waterman [1971]:

$$B_{\tau n}^i = \sum_{\tau' n'} T_{\tau n, \tau' n'}^i \, b_{\tau' n'}^i . \tag{8}$$

Substituting Equations (3), (4) and (7) in (2), we obtain

$$\sum_{\tau n} b_{\tau n}^i \text{ Re } \vec{\psi}_{\tau n}^i = e^{ik\hat{z}\cdot r_i} \sum_{\tau n} a_{\tau n} \text{ Re } \vec{\psi}_{\tau n}^i + \sum_{j\neq i}^{N} \sum_{\tau n} B_{\tau n}^j \, \vec{\psi}_{\tau n}^j \tag{9}$$

Since the field quantities are expanded with respect to centers of each scatterer, we obtain Equation (9) with basis functions expanded with respect to i-th and j-th centers. In order to express them with respect to a common origin 0_i, we employ the translation and addition theorems for the vector spherical functions [see, for example, Boström, 1980] which may be written in a compact form as follows

$$\vec{\psi}_{\tau n}(\vec{\rho}_j) = \begin{cases} \sum\limits_{\tau'n'} \sigma_{\tau n, \tau'n'}(\vec{\rho}_{ij}) \, \text{Re} \, \vec{\psi}_{\tau'n'}(\vec{\rho}_i) & ; \quad |\vec{\rho}_{ij}| > |\vec{\rho}_i| \\ \\ \sum\limits_{\tau'n'} R_{\tau n, \tau'n'}(\vec{\rho}_{ij}) \, \vec{\psi}_{\tau'n'}(\vec{\rho}_i) & ; \quad |\vec{\rho}_{ij}| < |\vec{\rho}_i| \end{cases} \qquad (10)$$

where $\vec{\rho}_{ij} = \vec{r}_i - \vec{r}_j$ is the vector connecting 0_j to 0_i, $\sigma_{\tau n, \tau'n'}$ is the translation matrix for the vector functions and $R_{\tau n, \tau'n'}$ is a matrix with spherical Hankel functions in $\sigma_{\tau n' \tau'n'}$ replaced by spherical Bessel functions.

Employing Equations (8) and (10) in (9) and using the orthogonality of the vector spherical basis functions, we obtain the following set of coupled algebraic equations for the exciting field coefficients $b_{\tau n}^i$:

$$b_{\tau n}^i = e^{ik\hat{z} \cdot \vec{r}_i} a_{\tau n} + \sum_{j \neq 1}^N \sum_{\tau n} \sum_{\tau'n'} \sigma_{\tau n, \tau'n'}(\vec{\rho}_{ij}) \, T_{\tau n, \tau'n'}^j \, b_{\tau'n'}^j \qquad (11)$$

From Equation (11), it can be seen that the exciting field coefficients of the i-th scatterer explicitly depend on the position and orientation of the other scatterers. In this paper, we consider a random distribution of spherical scatterers and the case when $N \to \infty$ and the volume occupied by the scatterers $V \to \infty$ such that $N/V = n_o$ is a finite number density. For such distribution, a configurational average of Equation (11) can be made over the positions of all scatterers [see Varadan et. al., 1981] with QCA [Lax, 1952] to arrive at an equation for the configurational average $<b_{\tau n}^i>_i$ of the exciting field coefficients with one scatterer fixed:

$$<b_{\tau n}^i>_i = e^{ik\hat{z} \cdot \vec{r}_i} a_{\tau n} + (N-1) \sum_{\tau n'} \sum_{\tau''n''} T_{\tau'n', \tau''n''}$$

$$\qquad (12)$$

$$\int_V p(\vec{r}_j | \vec{r}_i) \, \sigma_{\tau'n', \tau''n''}(\vec{\rho}_{ij}) \, <b_{\tau n}^j>_j \, d\vec{r}_j$$

where $p(\vec{r}_j|\vec{r}_i)$ is the two particle joint probability density. In obtaining the above equation, we have assumed that all the scatterers are identical.

We now assume that the average field $<b^i_{\tau n}>_i$ (the coherent field) propagates in a medium with an effective complex wave number $\vec{K} = (K_1 + iK_2)\hat{z}$ in the direction of the original incident field in the discrete random medium:

$$<b^i_{1\sigma m\ell}>_i = i^\ell\, Y_{1\sigma m\ell}\, e^{i\, \vec{K}\cdot\vec{r}_i} \tag{13}$$

$$<b^i_{2\sigma m\ell}>_i = i^\ell\, Y_{2\sigma m\ell}\, e^{i\vec{K}\cdot\vec{r}_i} . \tag{14}$$

Substituting Equations (13) and (14) in Equation (12) and invoking the extinction theorem to cancel the incident wave term in (12), we obtain the following equations for the unknown amplitudes $Y_{1\sigma m\ell}$ and $Y_{2\sigma m\ell}$

$$i^{n'} Y_{11\ell n'} = \sum_{n=1}^{\infty} \sum_{p=1}^{\infty} \sum_{m=|n-n'|}^{n+n'} i^p (-i)^m\, I_m$$

$$\left\{ Y_{11\ell p} \left[\left(T^{1\ell n}_{1\ell p}\right)^{11} \psi_{11}(n,n',m) + \left(T^{2\ell n}_{1\ell p}\right)^{21} \chi_{21}(n,n',m) \right] \right.$$

$$\left. + Y_{22\ell p} \left[\left(T^{1\ell n}_{2\ell n}\right)^{12} \psi_{11}(n,n',m) + \left(T^{2\ell n}_{2\ell p}\right)^{22} \chi_{21}(n,n',m) \right] \right\} ; \tag{15}$$

$$\ell\epsilon[0,n'] \quad ; \quad n'\epsilon[1,\infty]$$

$$i^{n'} Y_{22\ell n'} = \sum_{n=1}^{\infty} \sum_{p=1}^{\infty} \sum_{m=|n-n'|}^{n+n'} i^p (-i)^m I_m$$

$$\left\{ Y_{11\ell p} \left[\left(T_{1\ell p}^{1\ell n} \right)^{11} \chi_{12}(n,n',m) + \left(T_{1\ell n}^{2\ell n} \right)^{21} \psi_{22}(n,n',m) \right] \right.$$

$$\left. + Y_{22\ell p} \left[\left(T_{2\ell p}^{1\ell n} \right)^{12} \chi_{12}(n,n',m) + \left(T_{2\ell p}^{2\ell n} \right)^{22} \psi_{22}(n,n',m) \right] \right\} \quad ; \tag{16}$$

$$\ell \epsilon [0,n'] \; ; \; n' \epsilon [1,\infty]$$

where

$$I_m(K,k,c) = \frac{6c}{(ka)^2 - (Ka)^2} \; [2ka \; j_m \; (2Ka) \; h_m'(2ka)$$

$$-2Ka \; h_m(2ka) \; j_m'(2Ka)] + 24c \int_{x=1}^{\infty} x^2 [g(x)-1] \; h_m(kx) \; j_m(Kx) \; dx \tag{17}$$

$$\psi_{11}(n,n',m) = \psi_{22}(n,n',m) = -i^{n'-n+m} \left[\frac{(2m+1) \; (2n'+1)}{2n'(n'+1)} \right]$$

$$\left[\frac{n(n+1)}{n'(n'+1)} \right]^{1/2} \left[n(n+1) + n'(n'+1) - m(m+1) \right] \tag{18}$$

$$\begin{pmatrix} n & n' & m \\ 0 & 0 & 0 \end{pmatrix} \begin{pmatrix} n & n' & m \\ 1 & -1 & 0 \end{pmatrix}$$

$$\chi_{21}(n,n',m) = -\chi_{12}(n,n',m) = -i^{n'-n+m+1} \left[\frac{2(m+1)\ (2n'+1)}{2n'(n'+1)} \right]$$

$$\left[\frac{n(n+1)}{n'(n'+1)} \right]^{1/2} \left[\left\{ m^2-(n-n')2 \right\} \ \left\{ (n+n'+1)2-m^2 \right\} \right]^{1/2} \quad (19)$$

$$\begin{pmatrix} n & n' & m-1 \\ 0 & 0 & 0 \end{pmatrix} \begin{pmatrix} n & n' & m \\ 1 & -1 & 0 \end{pmatrix} .$$

In the above equation, $c = 4\pi\, n_o a^3/3$ is the effective spherical concentration. For plane waves propagating parallel to the rotational axis of symmetry of scatterers, only $\ell = 1$ contributes, and also only certain combinations of σ yield non-zero T-matrix elements which are used in Equations (15) and (16). In Equation (17), $g(x)$ is the pair correlation function which depends only on $|\vec{x}| = |\vec{\rho}_{ij}|$ due to translational invariance of the system under consideration. To obtain expressions for $g(x)$, a description of the interparticle forces is needed. In our statistics, the dielectric scatterers are assumed to behave like effective hard spheres of radius 'a' where 'a' is the radius of the circumscribing sphere, see Figure 1. Wertheim [1963] has obtained a series solution of the integral equation for the pair correlation function derived by Percus and Yevick [1958] for an ensemble of hard spheres. Throop and Bearman [1965] have used the Wertheim result and provided tabulated values of $g(x)$ as a function of x for several values of c. Plots of $g(x)$ vs x is shown in Figure 2.

At low values of concentration c, $g(x) \approx 1$, see Figure 2 and hence the integral in Equation (17) is negligible which results in a system of uncorrelated hard particles. This is what has been referred to as the well stirred approximation (WSA) and yields the 'hole correction integral' as outlined by Fikioris Waterman [1964] and by us earlier. If $g(x) > 1$, one can regard the

Equation (17) as a modified 'hole correction integral' which is of the same form as used by Twersky [1977, 1978].

Equations (15) and (16) are simultaneous linear homogeneous equations for the unknown amplitudes $Y_{\tau\sigma m\ell}$. For a nontrivial solution, we require that the determinant of the truncated coefficient matrix C vanishes, which yields an equation for the effective wave number $K = (K_1 + iK_2)$ in terms of k and the T-matrix of a scatterer. This is the dispersion relation for the scatterer filled medium. The real part of K relates to the phase velocity while the imaginary part relates to coherent attenuation in the medium.

3. NUMERICAL COMPUTATIONS

In the low concentration limit, $c \to 0$, it is well known that the single scattering approximation (SSA) is valid so that $Im(K/k)$ is given by

$$Im(K/k) = \frac{3}{8} c \frac{Q_{ext}}{ka} \tag{20}$$

where Q_{ext} is the normalized (with respect to πa^2) extinction cross section of a sphere of radius 'a'. An important problem is propagation in a rain medium where the single scattering approximation has been widely used. Indeed, even under very heavy rain, the concentration rarely exceeds 0.01 and is typically around 10^{-4}. We have compared our theory using WSA with Equation (20) for a distribution of spherical water drops of radius 0.1 cm with ka in the range $0.1 \leq ka \leq 3$. The refractive index, which is a function of frequency, is taken from Ray [1972]. In Figure (3), we show the attenuation constant γ defined as $4\pi \, Im(K)/Re(K)$ as a function of ka using the WSA for $c = 10^{-2}$, 10^{-3}, and 10^{-4} which is to be compared with Figure (4) which uses SSA. We note that

both solutions yield nearly identical results. In Figure (5), we show computation of γ vs concentration for different ka values using the WSA. Again the SSA is seemed to be excellent for the rain medium.

We now present computations for a random medium model used by Ishimaru [1981] for the optical propagation experiments. The scatterers are latex spheres of diameter 0.107μ immersed in water with incident wavelength λ = 0.6μ. In the Rayleigh limit, Twersky [1978b] has given an expression for Im(K/k) by considering the leading effects of the pair-correlation:

$$Im(K/k) = c(ka)^3 \left[\frac{\epsilon_r - 1}{\epsilon_r + 2} \right]^2 W \tag{21}$$

where ϵ_r is the relative dielectric constant and W is the packing factor given by

$$W = \frac{(1-c)^4}{(1+2c)^2} = 1 + 24c \int_0^\infty x^2 [g(x) - 1] \, dx \ . \tag{22}$$

In Figure (6), we show Im(K/k) as a function of concentration c using Equation (22) and the present theory employing the WSA, the P-YA and the Matern model. The Matern [1960] model is completely analytic and is valid for c < 0.125. We note that Equation (22) and the P-YA are identical while both the Matern model and the WSA fail for c ≈ 0.04, and in fact they give unphysical results for c > 0.125.

In Figure (7), we show the comparison between the computation and the two measured values at c = 0.01 and 0.10 given by Ishimaru [1981]. We note that the ka value is 0.56 and that multiple scattering effects are seemed to be important even at c = 0.01. The measured values at c = 0.01 and 0.1 are in

ACKNOWLEDGMENTS

BLANK PAGE

very good agreement with both the WSA and P-YA while the SSA consistently overestimates the effective coherent attenuation. Also, for c > 0.10 where measurements are not available at the present time, we feel that only the P-YA predicts the correct behavior of Im(K/k). In Figure (8), we show the variation of Im(K/k) with ka for c = 0.21 and compare the results using the SSA, the WSA and the P-YA. Values for the WSA for ka $\leq$ 0.75 are not shown since the solution fails [Im(K/k) < 0] in this region. However, as ka increases it appears that the WSA tends to merge with P-YA for ka $\geq$ 3.0. The SSA on the other hand predicts a higher attenuation than either the WSA or the P-Ya.

ACKNOWLEDGMENTS

REFERENCES

Boström, A. (1980), Multiple scattering of elastic waves by bounded obstacles, J. Acoust. Soc. Am., 67, 399-413

Bringi, V.N., T.A. Seliga, V.K. Varadan, and V.V. Varadan (1981), Bulk propagation characteristics of discrete random media, in Multiple Scattering of Waves in Random Media, edited by P.L. Chow, W.E. Kohler and G. Papanicolaou, 43-75, North-Holland Publishing Company, Amsterdam

Fikioris, J.G., and P.C. Waterman (1964), Multiple scattering of waves II. Hole corrections in the scalar case, J. Math. Phys., 5, 1413-1420

Lax, M. (1952), Multiple scattering of waves II. Effective field in dense systems, Phys. Rev., 85, 621-629

Matern, B. (1960), Meddn St. Skagsfork Inst. 49, 5-7

Percus, J.K., and Yevick, G.J. (1958), Analysis of classical statistical mechanics by means of collective coordinates, Phys. Rev., 110, 1-13

Talbot, D.R.S., and J.R. Willis (1980), The effective sink strength of a random array of voids in irradiated material, Proc. Roy. Soc. Lond., A, 370, 351-374

Twersky, V. (1978a), coherent electromagnetic waves in pair-correlated random distribution of aligned scatterers, J. Math. Phys., 19, 215-230

Twersky, V. (1978b), Multiple scattering of waves by periodic and random distributions, in Electromagnetic Scattering, edited by P.L.E. Uslenghi, 221-251, Academic Press, New York

Ray, P.S. (1972), Broadband complex refractive indices of ice and water, App. Optics, 11, 1836-1844

Varadan, V.K., V.N. Bringi and V.V. Varadan (1979), Coherent electromagnetic wave propagation through randomly distributed dielectric scatterers, Phys. Rev. D., 19, 2480-2489

Varadan, V.V., V.N. Bringi and V.K. Varadan (1981), Frequency dependent dielectric constants of discrete random media, The Ohio State University Research Foundation Report, 761261/711400, Columbus, Ohio

Waterman, P.C. (1971), Symmetry, unitarity and geometry in electromagnetic scattering, Phys. Rev. D., 3, 825-839

Wertheim, M.S. (1963), Exact solution of the Percus-Yevick integral equation for hard spheres, Phys. Rev. Lett., 10, 321-323
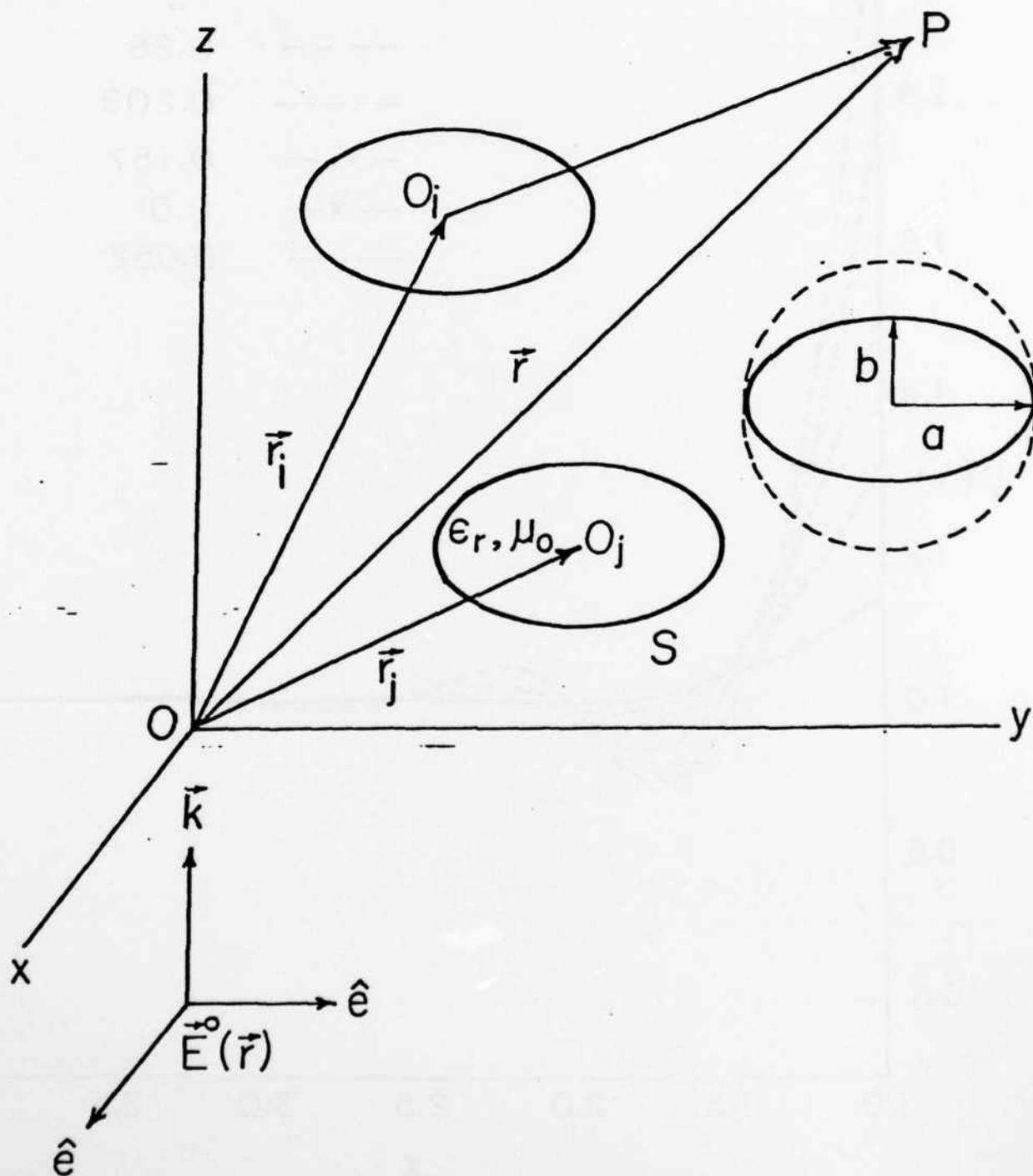
Figure 1. Geometry of randomly distributed and aligned scatterers
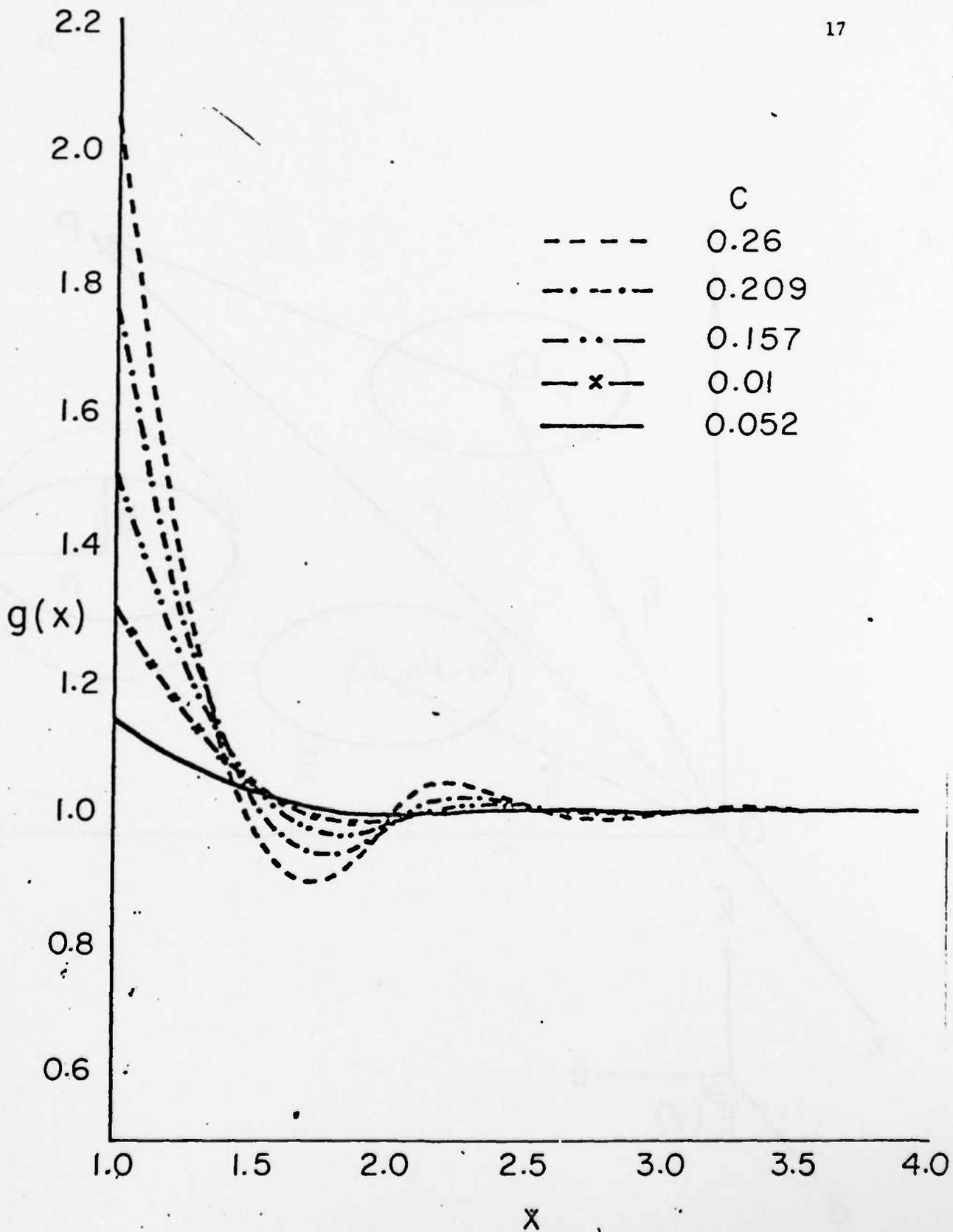
Figure 2. The Percus-Yevick pair correlation function for hard spheres
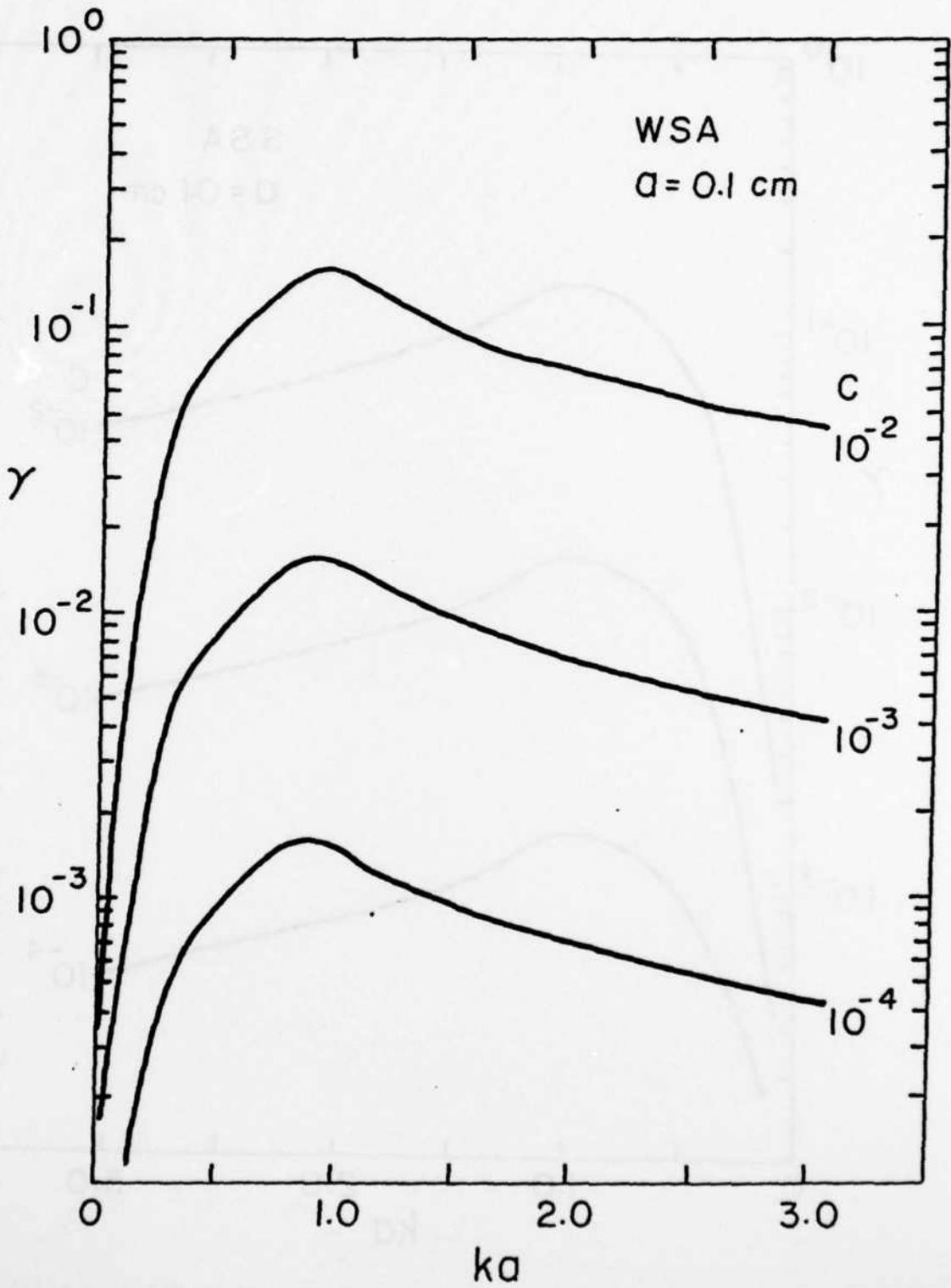
Figure 3. The coherent attenuation constant γ vs ka for $\epsilon_r = \epsilon_r(\lambda)$ using the WSA
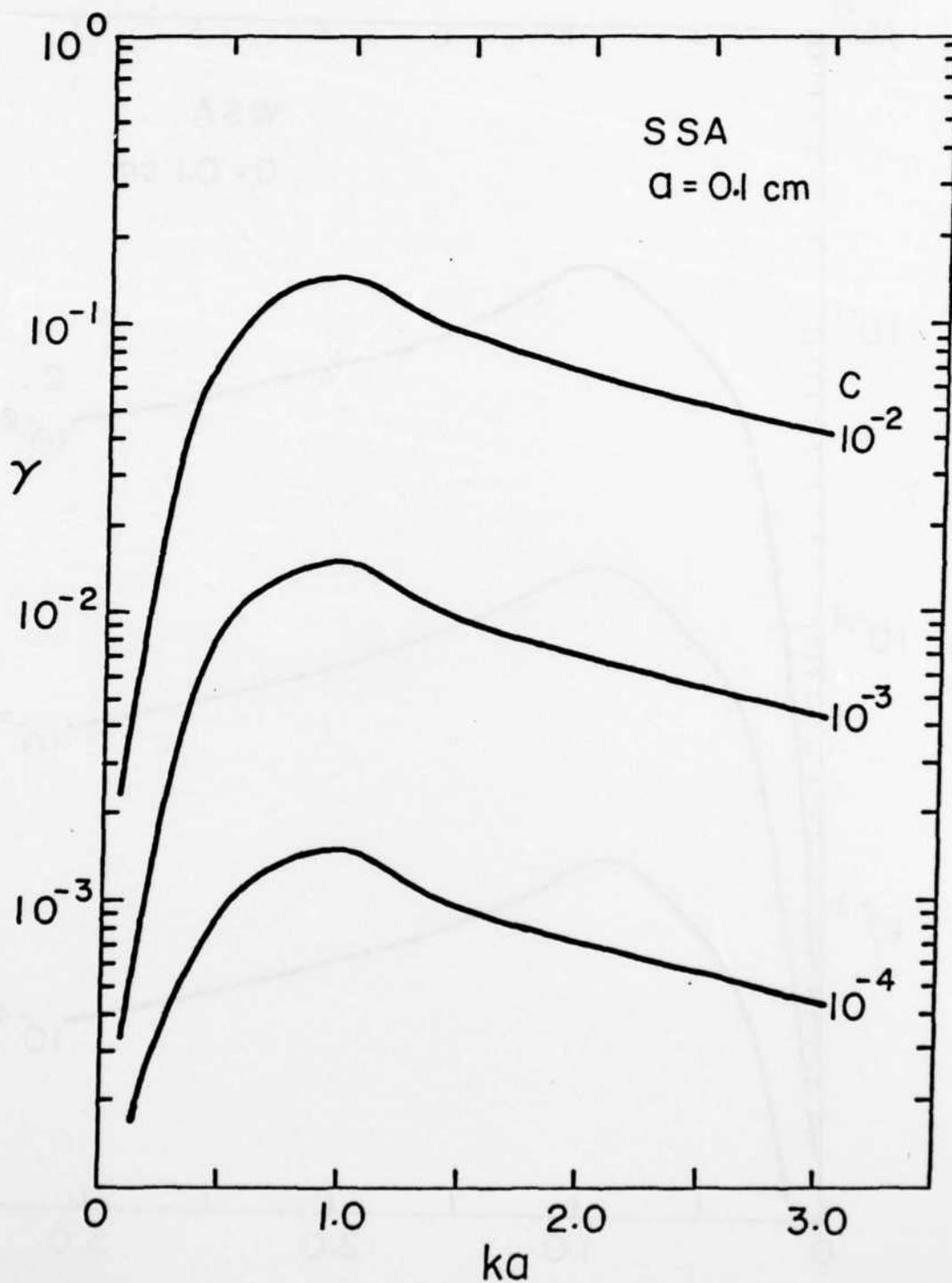
Figure 4. The coherent attenuation constant γ vs ka for $\varepsilon_r = \varepsilon_r(\lambda)$ using SSA
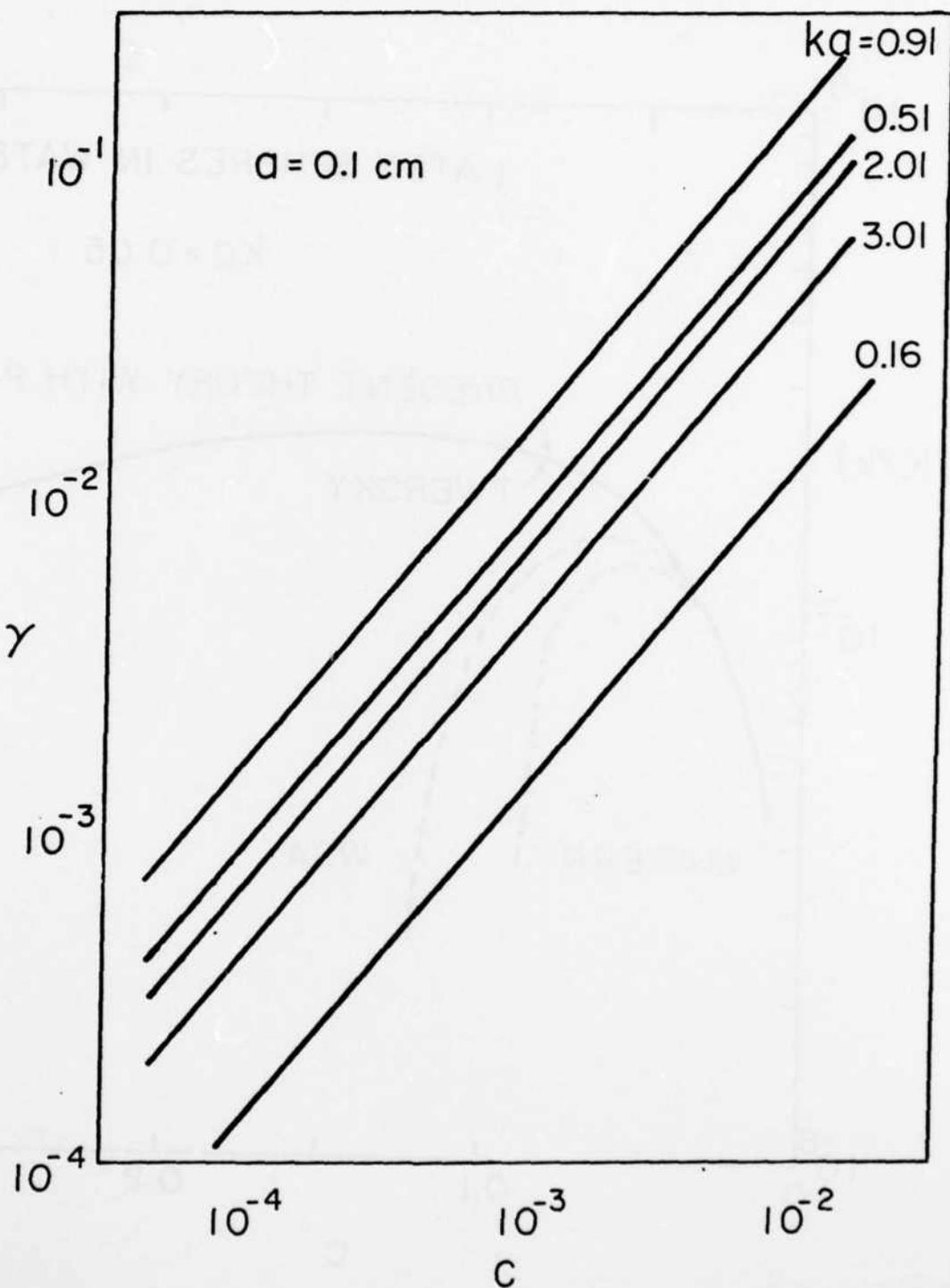
Figure 5. The normalized attenuation constant γ vs concentration c for different values of ka using the WSA
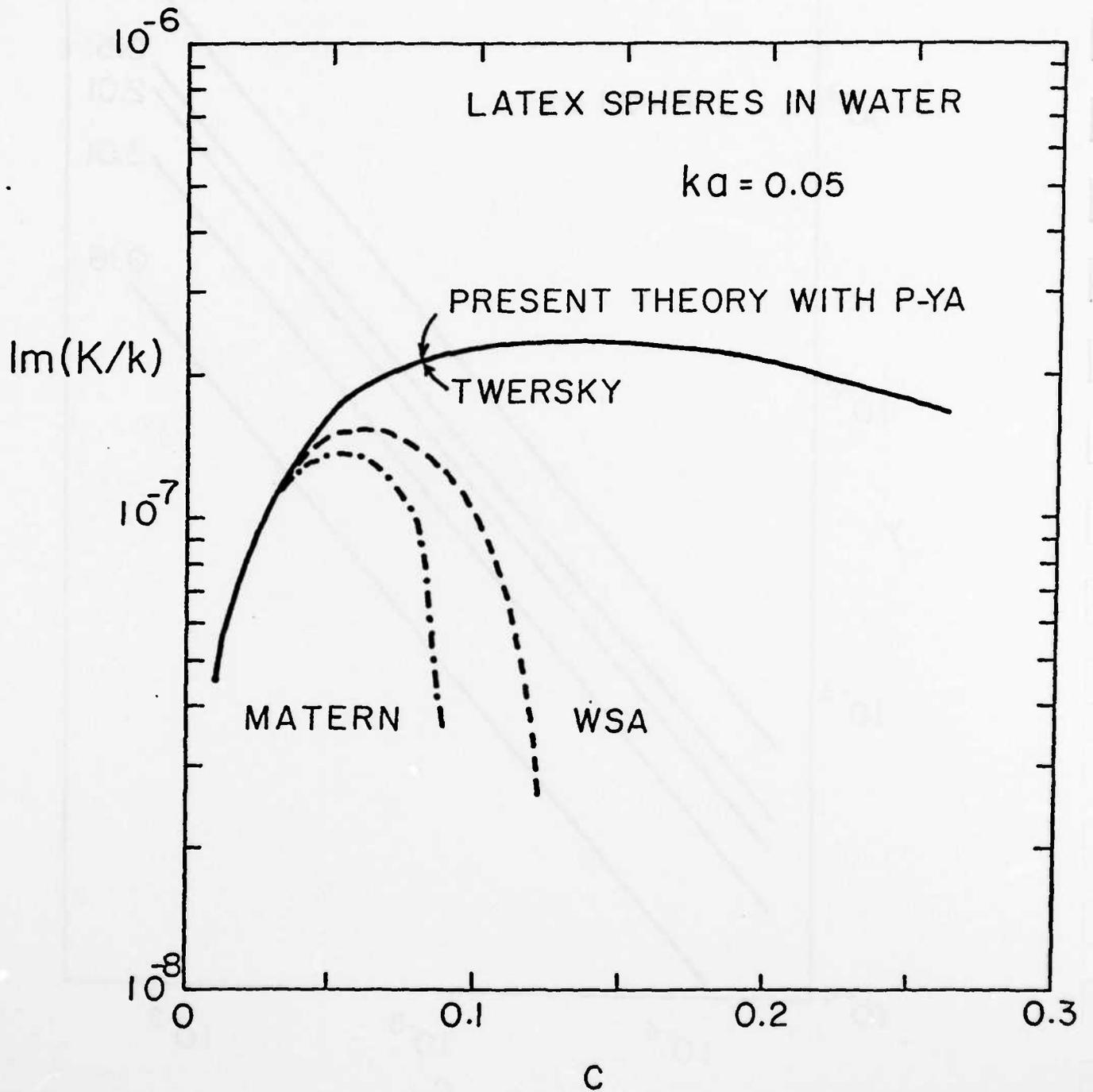
Figure 6. The coherent attenuation Im(K/k) vs concentration c at
ka = 0.05 for latex spheres in water
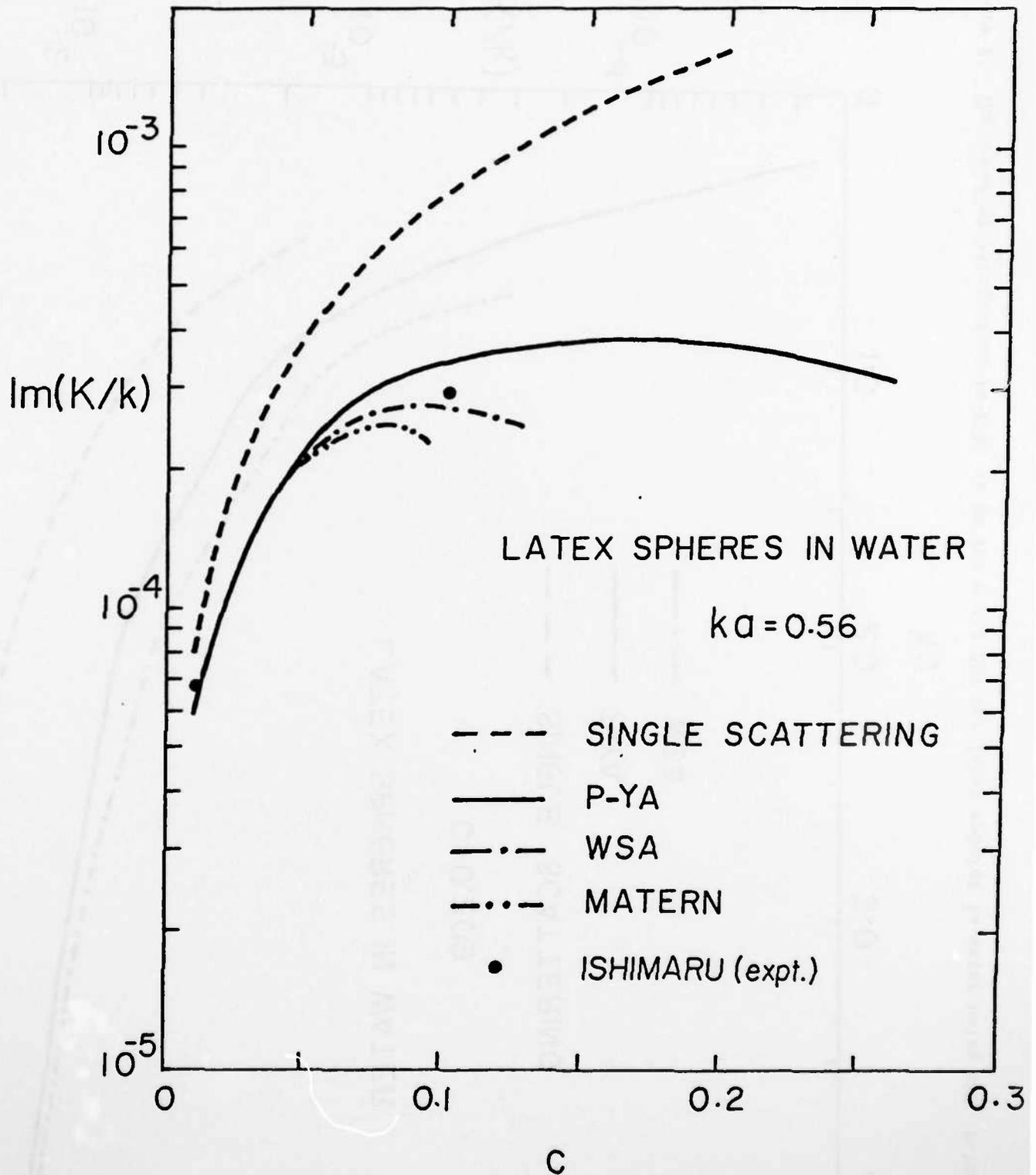
Figure 7. The coherent attenuation Im(K/k) vs concentration c at ka = 0.56
for latex spheres in water using different models of pair
correlation functions
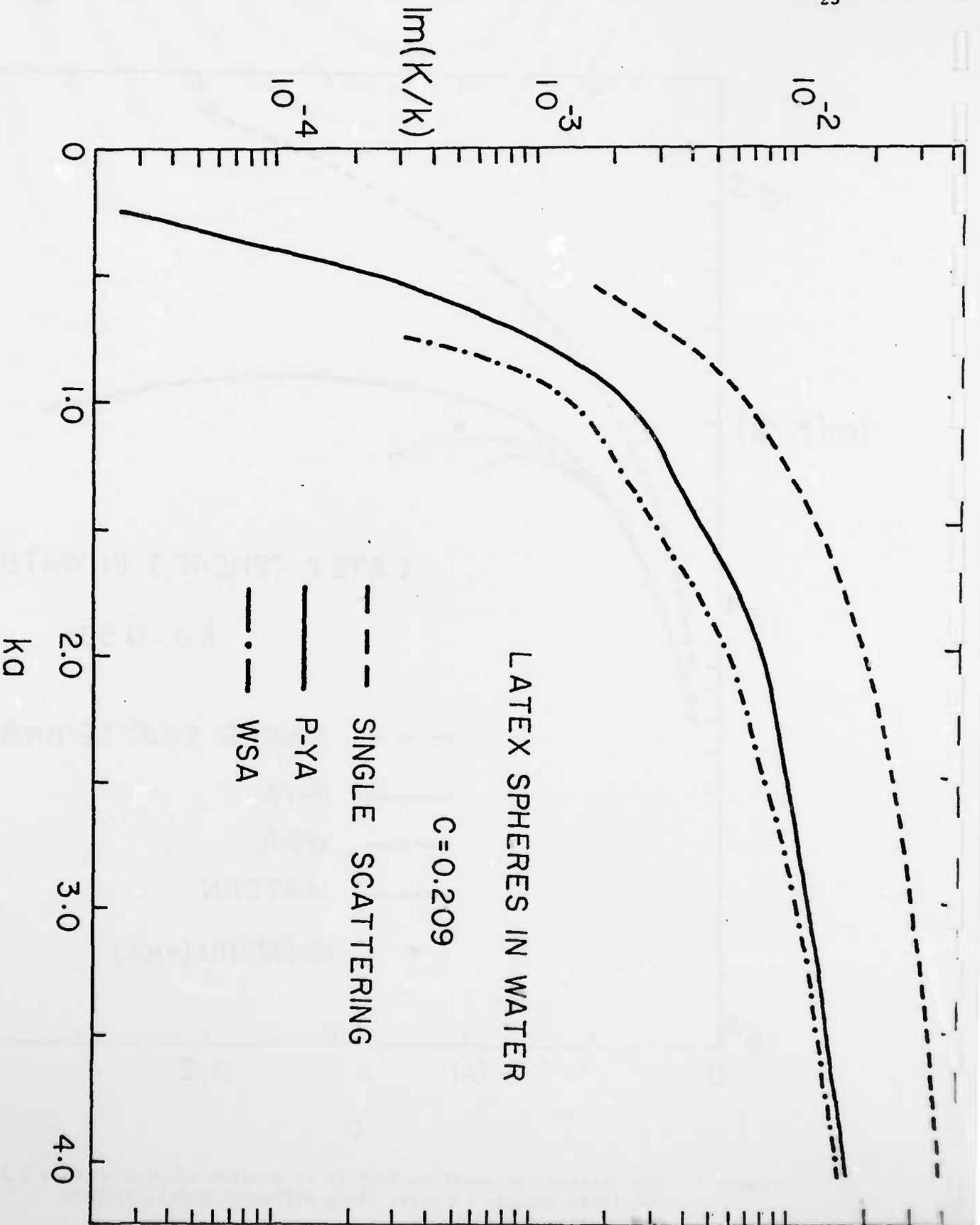
Figure 8. The coherent attenuation Im(K/k) vs ka for c = 0 209 for latex spheres in water using SSA, P-YA and WSA